Plant Stress 18 (2025) 100996

Contents lists available at ScienceDirect

Plant Stress

journal homepage: www.sciencedirect.com/journal/plant-stress

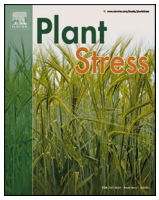

Cadmium-induced ER stress, autophagy and ethylene biosynthesis in leaves and roots of *Arabidopsis thaliana* and their dependence on stress intensity

Isabeau Vanbuel [a,#], Verena Iven [a,#], Thomas Depaepe [b], Martijn Heleven [c], Marijke Jozefczak [a], Karen Smeets [c], Luis E. Hernández [d], Els Prinsen [e], Dominique Van Der Straeten [b], Sophie Hendrix [a,*], Ann Cuypers [a,*]

[a] *Environmental Biology, Centre for Environmental Sciences, Faculty of Sciences, Hasselt University, Agoralaan Building D, B-3590 Diepenbeek, Belgium*
[b] *Laboratory of Functional Plant Biology, Department of Biology, Ghent University, K.L. Ledeganckstraat 35, B-9000 Ghent, Belgium*
[c] *Zoology, Biodiversity and Toxicology, Centre for Environmental Sciences, Faculty of Sciences, Hasselt University, Agoralaan Building D, B-3590 Diepenbeek, Belgium*
[d] *Laboratory of Plant Physiology, Department of Biology, Universidad Autónoma de Madrid, Cantoblanco, ES-28049 Madrid, Spain*
[e] *Department of Biology, University of Antwerp, Groenenborgerlaan 171, B-2020 Antwerp, Belgium*

A R T I C L E I N F O

Keywords:
Arabidopsis thaliana
Cadmium
Glutathione
Phytochelatin
Endoplasmic reticulum stress
Autophagy
1-aminocyclopropane-1-carboxylic acid

A B S T R A C T

Cadmium (Cd) pollution in soils and uptake by plant roots is a widespread problem, illustrating the requirement to enhance our knowledge of stress responses underlying its phytotoxicity. Acute Cd exposure induces an oxidative challenge in roots through the use of glutathione (GSH) for Cd-chelating phytochelatin (PC) production. To further uncover the acute Cd stress response of varying intensities, especially related to endoplasmic reticulum (ER) stress, autophagy, and the ethylene response, wild-type (WT) *Arabidopsis thaliana* were exposed to 2 and 5 μM Cd for 24 h. The dependence of these responses on stress intensity was explored by comparing Cd-sensitive *cad2–1* and *cad1–3* mutants with disturbed biosynthesis of GSH and PCs, respectively, to the WT. Indicative of ER stress, inositol requiring 1 (IRE1)-dependent *basic region/leucine zipper 60* (*bZIP60*) splicing and target genes were induced with increasing Cd stress in roots. In leaves, this response was already initiated at a lower stress intensity, but also reached its limit more quickly upon increasing stress. On the other hand, more severe Cd stress decreased transcript levels of two autophagy-inhibiting targets of IRE1-dependent decay of mRNAs (RIDD). Lower levels of these transcripts correlated with autophagy induction, suggesting a connection between ER stress and autophagy upon increasing Cd stress. Furthermore, while higher stress intensity stimulated the ethylene response, it also steered the ethylene precursor 1-aminocyclopropane-1-carboxylic acid (ACC) towards conjugation, forming malonyl-ACC. Lastly, this study demonstrates that the increased Cd sensitivity of the *cad2–1* mutant is mostly related to lower PC production rather than depleted GSH levels.

1. Introduction

The widespread distribution of cadmium (Cd) in soils is related to natural factors and anthropogenic processes such as (primarily historic) industrial activity and application of phosphate fertilisers to agricultural land and grassland (Ballabio et al., 2024). This non-essential metal can be taken up by plant roots via transport systems for essential elements, such as iron or zinc, after which it reaches shoots via the xylem (Sterckeman and Thomine, 2020; Zulfiqar et al., 2022). Cadmium uptake results in increased levels of reactive oxygen species (ROS) such as hydrogen peroxide (H_2O_2), of which the role teeters between signalling and damage (Cuypers et al., 2023). As Cd does not partake in redox reactions, its effect on the redox environment is indirect (Zulfiqar et al., 2022; Cuypers et al., 2023). As such, it induces the production of phytochelatins (PCs, i.e. $(\gamma\text{-Glu-Cys})_{2-11}$-Gly oligomers) that chelate metals via the thiol groups of their cysteine residues (Jozefczak et al., 2014; Seregin and Kozhevnikova, 2023). As these oligomers are produced from glutathione (GSH) via phytochelatin synthase (PCS, EC 2.3.2.15) (Seregin and Kozhevnikova, 2023), Cd-induced PC production is observed concomitantly with decreased root levels of this antioxidant (Jozefczak et al., 2014; Cuypers et al., 2023). Notably, it is this fast, transient root GSH depletion that was proposed to function as an

* Corresponding authors.
E-mail addresses: sophie.hendrix@uhasselt.be (S. Hendrix), ann.cuypers@uhasselt.be (A. Cuypers).
Shared first authors

https://doi.org/10.1016/j.stress.2025.100996
Received 30 April 2025; Received in revised form 30 July 2025; Accepted 14 August 2025
Available online 15 August 2025

H_2O_2-independent redox signal to induce early signalling responses during Cd stress, such as an ethylene response (Deckers et al., 2020; Iven et al., 2023).

The phytohormone ethylene is formed from the consecutive conversions of S-adenosylmethionine (SAM) to 1-aminocyclopropane-1-carboxylic acid (ACC) and of ACC to ethylene by ACC synthase (ACS, EC 4.4.1.14) and ACC oxidase (ACO, EC 1.14.17.4), respectively (Wang et al., 2002). In accordance with the previously proposed connection between Cd-induced changes in the oxidative environment and the ethylene response (Schellingen et al., 2015; Deckers et al., 2020; Iven et al., 2023), administration of GSH to *Zea mays* reduced Cd-induced ethylene emission in leaves and roots, even though root Cd concentrations were higher in the case of the simultaneous treatment compared to Cd treatment alone (Li et al., 2017). Correspondingly, ACC levels were also altered in *cad2-1* mutant *A. thaliana* leaves and roots compared to their WT counterparts following acute Cd exposure (Deckers et al., 2021). Next to being oxidised to ethylene, however, ACC can alternatively be conjugated to produce malonyl-, jasmonyl- or γ-glutamyl-ACC (Vanderstraeten and Van Der Straeten, 2017; Pattyn et al., 2021). While the in vivo significance of the last two conjugates is unclear, malonyl-ACC (MACC) formation may serve to control ethylene biosynthesis (Cao et al., 2024). There are also a few indications that Cd-stressed *A. thaliana* plants show enhanced ACC conjugation (Schellingen et al., 2014; Deckers et al., 2021). For instance, and in agreement with a connection between GSH and ethylene biosynthesis, Deckers et al. (2021) found higher conjugated ACC levels in the roots of Cd-exposed *cad2–1* mutant plants than in WT plants. Nevertheless, a reported change in Cd-induced ethylene biosynthesis or ACC conjugation in mutant plants with altered GSH concentrations may alternatively be related to the extent of Cd-induced PC production and Cd chelation rather than GSH as such. In agreement, ethylene production was higher in the PC-deficient *cad1–3* mutant compared to WT *A. thaliana* plants following Cd exposure (Chen et al., 2020), suggesting that the conversion of GSH to PC and the extent of Cd chelation are important determinants of the Cd-induced ethylene burst.

Next to the aforementioned connection between the redox environment and the ethylene response, Cd-induced oxidative changes are also tied to elevated protein oxidation in *A. thaliana* (Calero-Muñoz et al., 2019), and Cd also affects endoplasmic reticulum (ER) structure (Wierzbicka et al., 2007; Fan et al., 2011). Furthermore, even the ethylene response may link Cd to this organelle, as ER stress-related genes were found to be induced by ACC treatment and their expression also differed between leaves of WT and ethylene-insensitive *Solanum lycopersicum* (Czékus et al., 2022). Upon ER stress elicited by unfolded or misfolded proteins, multiple signalling branches are activated to induce an unfolded protein response of the ER (ER-UPR) in an attempt to relieve this stress. One of these signalling branches relies on the splicing of *basic region/leucine zipper 60* (*bZIP60*) mRNA by the ER stress sensor protein inositol requiring 1 (IRE1) (Cao et al., 2022). This process targets spliced bZIP60 to the nucleus rather than the ER, allowing it to induce target genes, such as the chaperone *binding protein 3* (*BiP3*) (Deng et al., 2011). Next to initiating this ER-UPR, IRE1 also contributes to the ER stress response by degrading mRNAs, which is referred to as the IRE1-dependent decay of mRNAs (RIDD) (Cao et al., 2022). Although previous research on Cd-mediated ER stress in plants has shown the induction of ER-UPR regulators and/or targets (Xi et al., 2016; De Benedictis et al., 2023; Song et al., 2023a; Li et al., 2024), RIDD stimulation following Cd stress remains, to the best of our knowledge, elusive. Nevertheless, the significance of the IRE1-RIDD pathway in stress responses is illustrated by its induction of autophagy (Bao et al., 2018), a process that was additionally suggested to be related to Cd-induced peroxisomal protein oxidation (Calero-Muñoz et al., 2019) and phytohormones such as ethylene (Liao et al., 2022).

During both micro- and macroautophagy, damaged cellular components are degraded in the vacuole. While this is achieved by tonoplast invagination in the first process, it occurs after the fusion of the tonoplast and the outer membrane of a double-membranous vesicle, i.e. an autophagosome, containing cellular material in the second process. Autophagosome formation is enabled by autophagy-related (ATG) proteins (Marshall and Vierstra, 2018). Among the ATG proteins, ATG8 is present on autophagosome membranes after conjugation to phosphatidylethanolamine (PE), forming ATG8-PE, and making ATG8 lipidation a useful parameter to study autophagy induction (Li et al., 2023). Although relatively less understood, several microautophagic processes also depend on ATGs (Sieńko et al., 2020). Autophagy is important not only during developmental processes but also during stress (Li et al., 2023). Correspondingly, Cd-induced autophagic structures were observed in various plant species (de Araújo et al., 2017; Gzyl et al., 2017; Yue et al., 2018; Calero-Muñoz et al., 2019; Huo et al., 2022; Meng et al., 2024), and *ATG10* overexpression was reported to enhance Cd tolerance of *Malus domestica* plants (Huo et al., 2022). At least in roots, it appears to depend on Cd stress intensity, as the number of autophagic structures and degree of ATG8 lipidation increased with higher Cd concentrations up to a certain level in *Brassica rapa* roots (Meng et al., 2024). Notably, the Cd-mediated effect on *ATG8* expression also differed between roots and leaves of *Citrus sinensis* (Fu et al., 2020), raising the question whether autophagy differentially occurs in both organs in response to Cd stress.

In this study, ER stress, autophagy, and the biosynthesis of ACC and ethylene were investigated in leaves and roots of *A. thaliana* plants after acute (24 h) Cd exposure. The dependence of these responses on Cd stress intensity was studied in WT plants exposed to increasing Cd concentrations (0, 2 or 5 μM $CdSO_4$). In parallel, these responses were validated using *cad1-3* and *cad2–1* mutants with increased Cd sensitivities (Howden et al., 1995a, 1995b) due to defective activities of PCS (Howden et al., 1995b) and the GSH biosynthetic enzyme γ-glutamylcysteine synthetase (GSH1, EC 6.3.2.2), respectively (Cobbett et al., 1998). While Cd-induced PC production is diminished in both mutants, GSH levels are only lower in the *cad2–1* mutant (Howden et al., 1995a, 1995b). In this way, this study expands our knowledge of the Cd stress intensity framework in leaves and roots, as well as the significance of GSH as PC precursor or in different functions during Cd stress.

2. Materials and methods

2.1. Plant cultivation, phenotypical follow-up and sampling

Wild-type (WT), the *cad1-3* mutant (Howden et al., 1995b) the *cad2-1* mutant (Cobbett et al., 1998), the *ire1a-2/ire1b-4* double mutant (kindly donated by Dr Olivier Lamotte from INRAE – Institut National de Recherche pour l'agriculture, l'alimentation et l'environment, France), and a Prom35S::GFP-ATG8H construct-carrying line (kindly provided by Dr Céline Masclaux-Daubresse from INRAE) of *Arabidopsis thaliana* (Col background) were used throughout this work. Unless stated otherwise, seeds were grown in hydroponics following seed surface sterilisation and dark stratification for two to three nights at 4 °C. Given that only one allelic variant is available for the *cad2* mutant (i.e. *cad2–1*), the *cad2–1* mutant will be referred to as *cad2* throughout the remainder of the text. A G-to-C substitution in the *cad1–3* mutant (Ha et al., 1999) and deletion of CGAAAG in the *cad2* mutant (Cobbett et al., 1998) were confirmed via sequencing following PCR amplification of the relevant DNA regions (Phusion™ Hot Start II DNA Polymerase, Thermo Fisher Scientific) (Supplemental Table S1). The hydroponics cultivation was performed as optimised previously (Smeets et al., 2008), with the exceptions that (1) Hoagland (pH 5.5–6.0) was modified to contain 0.08 μM $ZnSO_4{\cdot}7H_2O$, (2) purified, fine-grained sand was used as substrate in the hydroponic tubes and (3) a system of blue, red and far-red LED lamps (Philips Green-Power LED modules) were tuned to provide light at a photosynthetic photon flux density of averagely 165 μmol m^{-2} s^{-1} for 12 h daily. Day and night temperatures were set at 22 °C and 18 °C, respectively, and relative humidity was set at 65 %. The Hoagland solution was aerated continuously, starting from seven days after sowing, and

refreshed twice a week.

Three weeks after sowing, plants were kept under control conditions or exposed to 2 or 5 μM Cd by adding $CdSO_4$ to the Hoagland solution. After 24 h (or one week for the determination of thiobarbituric acid-reactive metabolites in WT and *cad* mutant plants), roots and rosettes (referred to as leaves throughout this work) were harvested, weighed, snap-frozen in liquid nitrogen and stored at −80 °C until further analyses (unless described otherwise). For long-term phenotypical monitoring of WT and *cad* mutant plants, the exposure period lasted one week. The number of leaves and rosette diameter were determined on the day of exposure and on the last day of exposure to calculate the number of leaves that emerged during the exposure period and to express the rosette diameter after the long-term exposure period relative to the diameter at the start of the exposure. Lastly, fresh weights were determined, and the percentage of dry weight (compared to fresh weight) was calculated after drying the samples at 60 °C.

2.2. Quantification of plant cadmium concentrations

At least 100 mg fresh weight was harvested. Leaves were first rinsed in dH_2O, while roots were consecutively incubated in 10 mM $Pb(NO_3)_2$ for 15 min at 4 °C and rinsed with dH_2O to chelate Cd adhering to their exterior. After drying the samples (60 °C), their weights were determined again. Afterwards, sample digestion was conducted by adding acids (70 % HNO_3 in three steps, 37 % HCl in one step) and heating the samples until evaporated. Finally, extracts were dissolved in 2 % HCl and analysed using inductively-coupled plasma-optical emission spectrometry [(ICP-OES), Agilent Technologies 700 Series] to determine root and leaf Cd concentrations. The resulting leaf Cd concentrations were divided by Cd concentrations of the corresponding roots to determine the Cd translocation factor. Spinach (SRM® 1570a, NIST®) was used as a reference (three technical replicates), while HNO_3 was used as a blank (three technical replicates).

2.3. Quantification of thiobarbituric acid-reactive metabolite levels as a proxy for lipid peroxidation

Frozen samples of at least 70 mg fresh weight were homogenised in 1 mL of cooled 0.1 % trichloroacetic acid (TCA, w/v). Following cold (4 °C) centrifugation of samples and blanks (i.e. 0.1 % TCA) at 20,000 x *g* for 10 min., 1 mL of 0.5 % thiobarbituric acid (TBA, w/v, in 20 % TCA) was added to 400 μL supernatant. Mixtures were incubated at 95 °C for 30 min, cooled and centrifuged again (20,000 x *g*, 4 °C, 10 min.), after which the absorbance of the resulting supernatants was measured in duplicate at 532 nm and corrected for non-specific absorbance at 600 nm. Lastly, the amount of TBA-reactive metabolites was calculated and normalised to fresh weight.

2.4. Quantification of the non-protein biothiols cysteine, glutathione and phytochelatin

A pre-cooled mortar and pestle were used to crush frozen samples of approximately 100 mg fresh weight in extraction buffer (5 % metaphosphoric acid, 1 mM EDTA, 0.1 % formic acid) and N-acetyl-l-Cys (NAC; internal standard) on ice. Following centrifugation (21,130 x *g*, 4 °C, 15 min), high performance liquid chromatography (HPLC) using the Chromaster HPLC System (VWR® Hitachi) and a Mediterranea Sea18 column [5 μm particle size, 25 × 0.46 cm (Teknokroma®)] was conducted as described previously (Sobrino-Plata et al., 2014). Biothiols were detected as 5-mercapto-2-nitrobenzoate derivatives (max. absorbance of 412 nm) following their post-column derivatisation with Ellman's reagent [1.8 mM 5,5′-dithiobis(2-nitrobenzoic acid) in K-P buffer of 300 mM KH_2PO_4 and 15 mM K_2-EDTA at pH 7.5] delivered via Waters™ Reagent Manager. Biothiol derivatives in samples were compared to those from standards for Cys (Thermo Fisher Scientific), GSH (Thermo Fisher Scientific) and PCs (Eurogentec®). Using NAC as the internal standard, the amount (nmol) of each biothiol in a sample was calculated and normalised to fresh weight.

2.5. Gene expression analysis

After homogenising frozen samples of approximately 50 mg in the Mixer Mill MM 400 (Retsch), their RNA was extracted using the RNAqueous™ Total RNA Isolation Kit (Invitrogen™, Thermo Fisher Scientific). Purity and concentrations of RNA were determined using the NanoDrop® ND-1000 Spectrophotometer (Thermo Fisher Scientific) to enable cDNA synthesis from an equal RNA input of 1 μg. Residual genomic DNA was removed from the RNA extracts using the TURBO DNA-*free*™ kit (Invitrogen™, Thermo Fisher Scientific) prior to cDNA synthesis. Afterwards, cDNA was synthesised from RNA using the PrimeScript™ RT Reagent Kit (Perfect Real Time, Takara Bio) and diluted tenfold in 1/10 TE buffer (1 mM Tris–HCl, 0.1 mM Na_2-EDTA, pH 8.0) before storage at -20 °C.

Gene expression levels were determined via quantitative PCR (qPCR) using the QuantStudio™ 3 Real-Time PCR System (Applied Biosystems™, ThermoFisher Scientific) and the QuantiNova® SYBR® Green PCR Kit (Qiagen). Primers for genes of interest and reference genes were designed using Primer3 (Rozen and Skaletsky, 2000), and *in silico* predictions regarding their sequence specificity were made using TAIR BLAST (The Arabidopsis Information Resource, https://www.arabidopsis.org/tools/blast/), except for *bZIP60s* and unspliced *bZIP60* (*bZIP60us*) primers that were designed as reported previously (Xi et al., 2016) (Supplemental Table S1). Following their design, primers were subjected to efficiency testing using a twofold dilution series of a pooled cDNA sample. Each qPCR contained a mixture of Quantinova® SYBR® Green PCR Master Mix (5 μL), ROX™ reference dye (0.05 μL), tenfold-diluted cDNA (2 μL), forward primer and reverse primer, filled up to a final volume of 10 μL with RNase-free H_2O. Primers were added at a final concentration of 300 nM to each reaction, unless stated otherwise in Supplemental Table S1. An initial denaturation was performed at 95 °C for 2 min, which was followed by 40–60 cycles of two steps at 95 °C (5 s) and 60 °C (12 s) and ended with the generation of a melting curve (95 °C for 15 s, 60 °C for 1 min, 95 °C for 15 s, 60 °C for 15 s). Subsequently, relative expression levels were calculated using the $2^{-\Delta Cq}$ method and normalised against the geometric mean of at least three GrayNorm-selected reference genes [Supplemental Table S1, Remans et al. (2014)]. All additional technical information regarding the conducted gene expression analysis is given in Supplemental Table S2 according to the Minimum Information for Publication of Quantitative Real-Time PCR Experiments (MIQE) guidelines (Bustin et al., 2009).

2.6. Determination of autophagy-related 8 lipidation

To determine ATG8 lipidation, protein extraction and immunoblotting were largely performed as described previously (Kacprzak and Van Aken, 2023). In short, frozen samples of approximately 150 mg were homogenised in extraction buffer [50 mM Tris–HCl pH 7.5, 150 mM NaCl, 0.5 mM Na_2-EDTA, cOmplete™ Mini EDTA-free Protease Inhibitor Cocktail (Roche)] using a pre-cooled mortar and pestle on ice. Following centrifugation (1000 x *g*, 5 min, 4 °C), total protein concentration was determined using the Bio-Rad Protein Assay and bovine serum albumin (BSA) as protein standard. Equally concentrated protein samples were 1/1 diluted in sample buffer (recipe for 2X Laemmli Sample Buffer from Bio-Rad) containing 2-mercaptoethanol (5% v/v), boiled (95 °C for 5 min) and cleared (600 x *g*, 4 °C, 1 min). Afterwards, protein separation was performed at 4 °C using 15 % SDS-PAGE containing 6 M urea to enable sufficient distinction between ATG8 and faster-migrating ATG8-PE (Yoshimoto et al., 2004). Separated proteins were transferred to a 0.45 μm nitrocellulose membrane (Amersham™ Protran®, Cytiva™) using wet transfer (4 °C) and subsequently visualised using Ponceau S Staining Solution (Cell Signaling Technology®). Following

destaining in TBS (20 mM Tris, 150 mM NaCl), membranes were consecutively blocked [5 % (w/v) milk in TBS, 75 min] and incubated overnight with 1/2000-diluted anti-ATG8 (AS14 2769, Agrisera) in 5 % (w/v) milk in TBS at 4 °C. Afterwards, blots were incubated with horse radish peroxidase (HRP)-conjugated secondary antibody [1/50,000 goat anti-rabbit (AS09 602, Agrisera) in 5 % (w/v) milk in TBS, 1 h, RT]. Wash steps following antibody incubation were performed using TBS containing 0.1 % (v/v) Tween-20. Finally, bots were visualised using AgriseraECL SuperBright (Agrisera) and the ImageQuant™ LAS 4000 mini (GE Healthcare). Peak heights of ATG8 and ATG8-PE bands were quantified in ImageJ 1.53c [National Institutes of Health, (Schneider et al., 2012)] and used to calculate the ATG8 lipidation degree per sample, given as: ATG8-PE/(ATG8+ATG8-PE).

2.7. Visualisation of autophagic structures

Prom35S::GFP-ATG8H *A. thaliana* plants were grown in hydroponics and exposed to 0 or 5 μM $CdSO_4$ as described previously (Section 2.1). Additional treatment with 0.5 μM concanamycin A started 2 h prior to imaging. Root tips (lower 1 cm of the primary root) were cut and consecutively rinsed and mounted in MilliQ H_2O. Inverted confocal laser scanning microscopy was performed using the LSM 900 (Zeiss) with a 40X objective (LD C-Apochromat 40x/1.1 W Korr UV VIS IR) to detect GFP-ATG8H puncta following excitation with a 488 nm laser. The pinhole was set to 1 airy unit (40 μm), and imaging settings were kept constant across all samples within each experiment. Visualised GFP-ATG8H puncta (detection at 450-700 nm) were counted in trichoblasts with early root hair formation to minimise variation due to cell type and developmental stage. Fluorescence was used solely as a qualitative visualisation tool to enable quantification of vesicles based on their presence and distribution. As such, intensity measurements were not performed, as they are expected to be subject to inherent variability in, for example, live root mounting, sample positioning and differences in intrinsic autofluorescence levels.

2.8. Quantification of ethylene production

Rockwool-based plant cultivation for the quantification of ethylene production was performed as described previously (Schellingen et al., 2014), with the exception that three plants were grown per plug and that Hoagland solution was prepared as described for the hydroponics experiments in the current study. Light, day/night rhythm and relative humidity were set to the same conditions as described for the hydroponics cultivation described in Section 2.1. Transfer of plants to the glass cuvette system, exposure to Cd (albeit to different concentrations, i.e. 0, 25, 100 or 250 μM $CdSO_4$), calibration and photo-acoustic ethylene detection by the ETD-300 (Sensor Sense) were additionally performed according to Schellingen et al. (2014). Data were normalised to leaf fresh weight, which was determined immediately following ethylene detection.

2.9. Quantification of 1-aminocyclopropane-1-carboxylic acid levels

Standards for 1-aminocyclopropane-1-carboxylic acid (ACC) and malonyl-ACC (MACC) were purchased (Merck) and synthesised according to Cao et al. (2024), respectively. Leaf and root samples of at least 30 mg were homogenised under frozen conditions and incubated with 1 mL 80 % (v/v) methanol, spiked with internal standards for ACC and methionine [d_4-ACC (Olchemim Ltd, Olomouc) and d_3-methionine (Merck)] at 1 nmol each. Overnight incubation at −20 °C was followed by the addition of 0.5 mg OASIS HLB solid phase extraction sorbent (Waters™) per 400 μL extract to bind pigments and cold centrifugation (15,900 x *g*, 4 °C, 5 min). A Chromafil® AO-20/3 filter [nylon, 0.2 μm pore size, 3 mm diameter (Macherey-Nagel)] was used to filter the resulting supernatant, after which the samples were dried under a nitrogen stream (TurboVap®, Biotage). Samples re-dissolved in 70 μL 10 % (v/v) methanol were lastly analysed via electrospray ionisation ultra-high-performance liquid chromatography tandem mass spectrometry (ES(+)UPLC-MS/MS), as described by Cao et al. (2024), using an ACQUITY UPLC® BEH Amide Column [1.7 μm, 15 × 0.21 cm (Waters™)] and an ACQUITY TQD Tandem Quadrupole UPLC/MS/MS System (Waters™). Next to free ACC, the same extracts were used to determine MACC (Cao et al., 2024). To this end, a BEH C18 VanGuard pre-column [130 Å, 1.7 μm, 2.1 mm x 5 mm (Waters™)] was combined with a reverse-phase Bridged Ethylsiloxane/silica Hybrid (BEH) C18 Column [130 Å, 1.7 μm, 2.1 mm x 50 mm (Waters™)].

2.10. Statistical analysis

Statistically significant outliers were detected using Grubbs' test (GraphPad Outlier calculator, https://www.graphpad.com/quickcalcs/grubbs1/). All remaining statistical analyses were performed in RStudio (Posit Software based on R, The R Foundation for Statistical Computing). The assumptions for normality and homoscedasticity were verified using the Shapiro-Wilk and Bartlett tests, respectively. If required to meet these assumptions, data were transformed (square root, inverse, exponent, logarithm). Gene expression data were routinely transformed logarithmically. Data between two groups were compared using (1) a two-sample *t*-test if the assumptions were met, (2) a Wilcoxon rank sum test if the normality assumption was not met or (3) a Welch two-sample *t*-test if the homoscedasticity assumption was not met. A one- or two-way ANOVA with post-hoc Tukey HSD test was used for a one-factor or two-factor experimental design, respectively. However, a non-parametric Kruskal-Wallis rank sum test and post-hoc Wilcoxon rank sum test were used when one or both assumptions were not met for these factorial designs. All tests were subjected to a significance level of 0.05.

Furthermore, the geometric mean of the normalised relative *AT5G01870* and *ROSY1* expression was correlated with either the geometric mean of the normalised relative *ATG8A-I* expression or the degree of ATG8 lipidation using the non-parametric Spearman's rank correlation method. The gene expression data were log_2-transformed prior to their correlation to enhance data visualisation. As the sample size was not sufficiently expansive to conduct partial correlations (due to a risk of overfitting), the correlations were additionally performed on subsets of the data to estimate the effect of a certain variable on the correlation.

3. Results

This research aimed to gain insight into the occurrence of different responses related to ER stress, autophagy, ACC and ethylene in leaves and roots of plants acutely experiencing Cd stress at varying intensities during their vegetative growth stage. Therefore, hydroponically grown, three-week-old WT *A. thaliana* plants were exposed to 2 and 5 μM $CdSO_4$ to induce stress that will respectively be referred to as mild and moderate throughout this manuscript. In addition, Cd stress was intensified by including the Cd-sensitive *cad1-3* and *cad2* mutants in this research.

3.1. The effect of cadmium on growth and lipid peroxidation is concentration-dependent and worsens in the cad2 and cad1–3 mutants

To explore the stress intensity elicited by multiple Cd concentrations in WT and *cad* mutant plants, their growth and levels of TBA-reactive metabolites (TBArm), as a measure for lipid peroxidation, were determined after long-term (one week) Cd exposure. In line with a concentration-dependent effect of Cd on plant growth, we found that 5 μM Cd, but not 2 μM Cd, significantly reduced leaf and root fresh weights of WT plants (Fig. 1A). This appears, at least partly, linked to disturbed water homeostasis, as this Cd concentration did not affect the dry weights of these organs (Supplemental Figure S1B). Furthermore, 5 μM Cd also hampered the increase in rosette diameter during the exposure

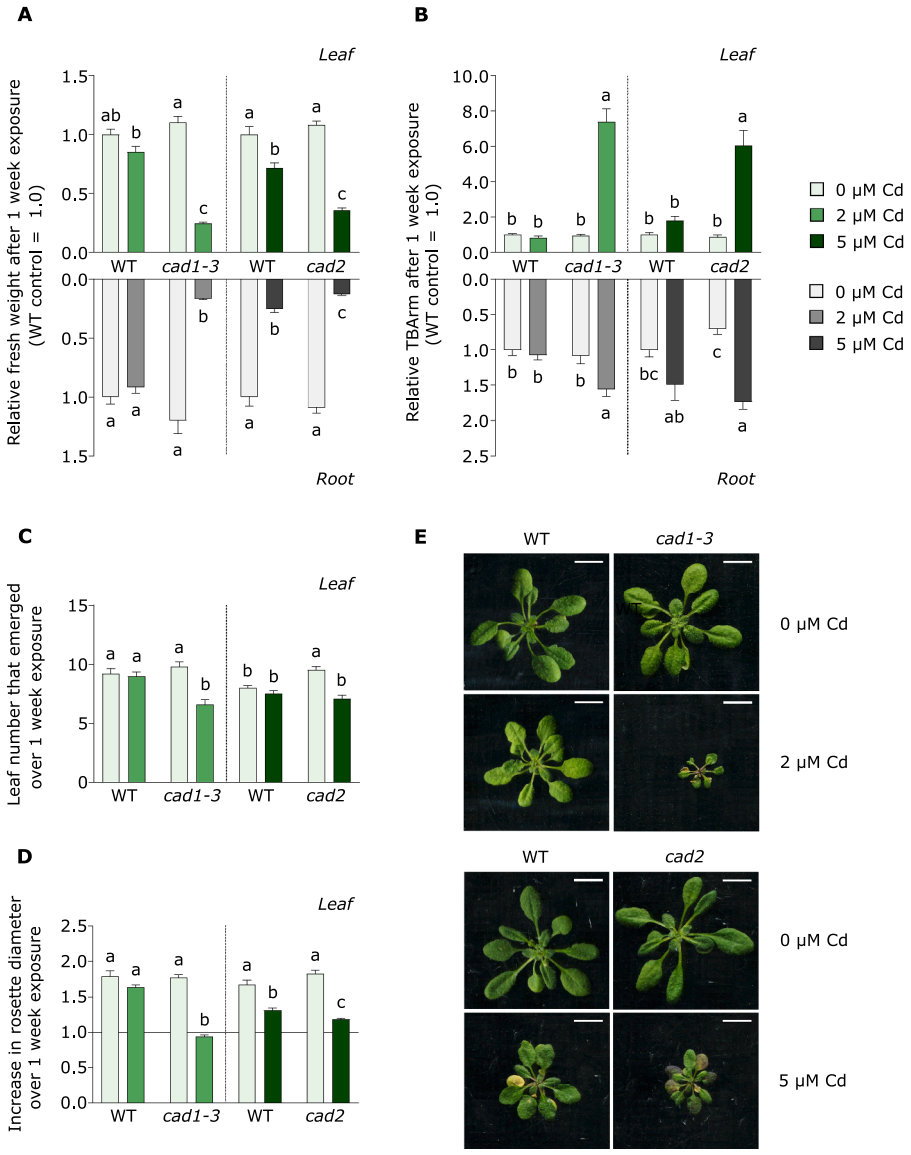

Fig. 1. Biometric and stress-related parameters of hydroponically grown, four-week-old wild-type (WT) as well as cadmium (Cd)-sensitive *cad1-3* and *cad2* mutant *Arabidopsis thaliana* plants after exposure to 0, 2 or 5 µM $CdSO_4$ for one week. **(A)** Leaf and root fresh weight (mg) as well as **(B)** concentrations of thiobarbituric acid-reactive metabolites (TBArm) were assessed solely after one week of Cd exposure and were set relative to the control (0 µM $CdSO_4$) of the WT. **(C)** The number of leaves that emerged during the exposure period was determined by subtracting the leaf number before the exposure from the leaf number after the exposure. **(D)** The increase in rosette diameter over the exposure period was determined by setting the rosette diameter after the exposure relative to the rosette diameter prior to exposure, with a value of 1.0 reflecting the situation where there was no increase in rosette diameter over the exposure period. Data are shown as the average + SE of at least **(A, C-D)** nine or **(B)** five biological replicates. Statistically significant differences, determined between each mutant and its corresponding WT per organ, are depicted using different letters (parametric two-way ANOVA with post-hoc Tukey HSD test or non-parametric Kruskal-Wallis rank sum test with post-hoc Wilcoxon rank sum test, $p < 0.05$). Lastly, rosette images are depicted in **(E)**, where the scale bar represents 1 cm.

period and induced chlorosis (Figs. 1D-E). Despite this effect on rosette diameter, a similar number of leaves still developed during this long-term exposure period in control- and Cd-exposed WT plants (Fig. 1C), indicating that new leaf formation is prioritised over leaf expansion.

Next to the concentration-dependent effect of Cd on WT plants, we confirmed the increased sensitivity of the *cad1-3* mutant compared to the WT, as Cd-induced effects on growth parameters were largely only evident in the mutant, but not in the WT, after exposure to 2 µM Cd (Fig. 1, Supplemental Figure S1B). Given that the *cad1–3* mutant did not further expand its rosette diameter after exposure to this concentration (Fig. 1D), it was only exposed to 2 µM Cd throughout this research. Therefore, in order to induce a more severe stress response compared to WT plants that were exposed to the highest Cd concentration (i.e. 5 µM Cd), the *cad2* mutant was used. While this mutant was still able to slightly increase its rosette diameter during prolonged exposure to 5 µM Cd, its increased sensitivity compared to WT plants exposed to this Cd concentration was also evidenced by its more severe leaf discolouring as well as its more pronounced reductions in fresh weight, root dry weight, leaf emergence and rosette diameter expansion compared to the WT (Fig. 1, Supplemental Figure S1B). Lastly, the high sensitivity of the Cd-exposed *cad* mutants compared to their WT plants was also corroborated by their increases in lipid peroxidation, which were especially pronounced in leaves compared to roots (Fig. 1B).

Taken together, these results validate the gradual increase in Cd stress by (1) elevating the applied Cd concentration in WT plants and (2) employing *cad1–3* and *cad2* mutants that are more sensitive to Cd than their WT counterparts. As Cd-induced signalling occurs early after the exposure (Deckers et al., 2020), this gradual stress intensity framework

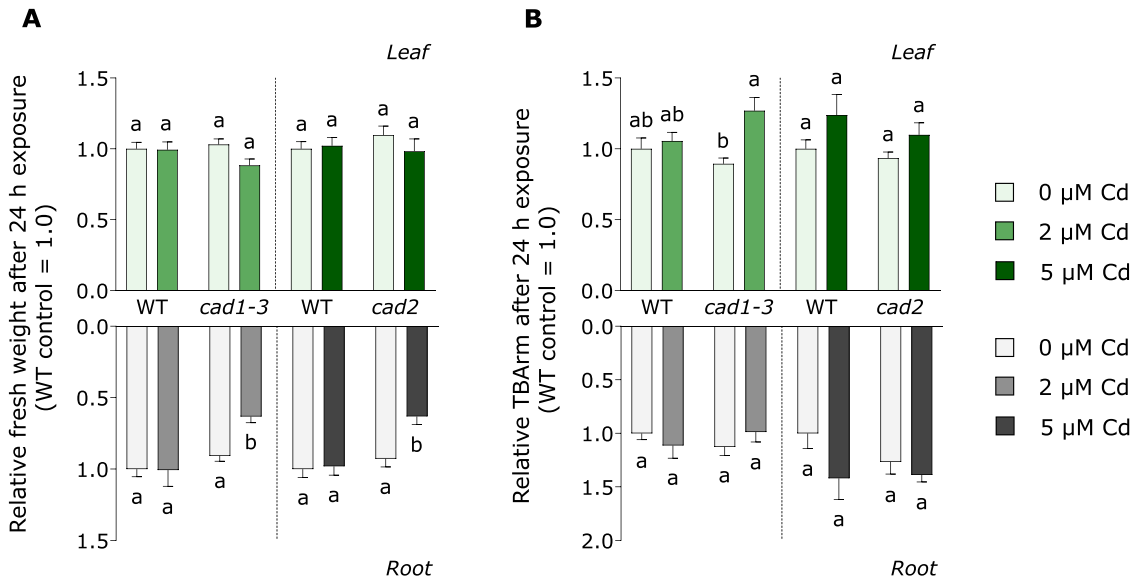

Fig. 2. **(A)** Relative fresh weight and **(B)** relative concentration of thiobarbituric acid-reactive metabolites (TBArm) in leaves and roots of three-week-old, hydroponically grown wild-type (WT) as well as cadmium (Cd)-sensitive *cad1–3* and **cad2** mutant *Arabidopsis thaliana* plants exposed to 0, 2 or 5 µM $CdSO_4$ for 24 h. Data, set relative to the control condition (0 µM $CdSO_4$) of the WT, are depicted as the average + SE of at least (A) ten or (B) five biological replicates. Statistically significant differences between each mutant and its corresponding WT per organ are indicated using different letters (two-way ANOVA with post-hoc Tukey HSD test, $p < 0.05$).

was next employed in a short-term setting (24 h) to investigate how stress intensity determines the signalling responses related to ER stress, autophagy and ethylene in leaves and roots of Cd-exposed plants. While short-term Cd exposure did not yet affect the weights of WT leaves and roots, reduced fresh weights and slightly decreasing trends in dry weight were observed for roots of the *cad* mutant plants (Fig. 2A; Supplemental Figure S1A). In addition, the especially high Cd sensitivity of the *cad1–3* mutant was further evidenced by its increased leaf TBArm level after exposure to 2 µM Cd (Fig. 2). As differences in Cd stress intensity could also be linked to differences in Cd uptake, Cd concentrations were compared between WT plants and the Cd-sensitive genotypes. In WT plants exposed to 2 or 5 µM Cd, the distribution of this metal was largely similar between leaves and roots after 24 h exposure (Table 1). Notably, the Cd translocation factor was significantly lower in *cad1-3* and *cad2* mutant plants compared to WT plants. Accordingly, Cd concentrations in the roots of these mutants were higher compared to those of their WT counterparts, whereas the opposite was observed for the leaves (Table 1).

3.2. *The extent of cadmium stress is reflected by altered biothiol levels and a transcriptional response indicative of oxidative stress*

The Cd-sensitive mutants used in this research are known to have altered GSH and PC levels (Howden et al., 1995a, 1995b). To confirm this and determine how they are affected by different Cd concentrations, the levels of cysteine, GSH, and PCs – as major metabolites containing thiol (-SH) groups, hereafter often referred to as biothiols – were determined in WT, *cad2* and *cad1-3* mutant *A. thaliana* plants exposed to 0, 2 or 5 µM Cd for 24 h. Furthermore, the extent of oxidative stress was also estimated by determining the expression of five genes that were previously identified as hallmarks of oxidative stress (Gadjev et al., 2006). Exposure of WT plants to 2 µM Cd resulted in a fast increase in total biothiol levels due to higher concentrations of cysteine and PCs in leaves as well as all three measured biothiols in roots (Fig. 3). When the Cd concentration increased to 5 µM, the elevated biothiol levels were a result of higher levels of PCs in leaves and of both cysteine and PCs in roots (Fig. 3). The strong PC induction, which reached levels within a similar order of magnitude in Cd-exposed WT plants after 2 and 5 µM Cd treatment, highlights its importance during the Cd stress response of both lower and higher intensity (Fig. 3C).

The *cad2* mutant generally showed lower total biothiol levels under control and Cd-exposed conditions in comparison to the WT (Fig. 3D). This resulted from decreased concentrations of GSH and its downstream product, PCs, although PC biosynthesis was still induced to some extent in Cd-exposed *cad2* mutant leaves and roots (Fig. 3B-C). While leaf GSH concentrations were not affected by short-term Cd treatment in the *cad2* mutant, root GSH levels were significantly depleted (Fig. 3B). In line with its root GSH depletion and weaker PC production, this mutant showed an accumulation of the GSH building block cysteine in response to 5 µM Cd (trend for roots, $p = 0.057$) (Fig. 3A). The *cad1-3* mutant, on the other hand, was confirmed to be PC-deficient under control and Cd-exposed conditions (Fig. 3C), even though its total biothiol concentrations remained similar to those of WT plants (Fig. 3D). This was attributed to the accumulation of PC precursors cysteine and GSH,

Table 1
Concentrations of cadmium (Cd) (mg kg^{-1} dry weight) in leaves or roots and the root-to-leaf translocation factor of Cd in hydroponically grown, three-week-old wild-type (WT) as well as Cd-sensitive *cad1-3* and *cad2* mutant *Arabidopsis thaliana* plants after exposure to 2 or 5 µM $CdSO_4$ for 24 h.

2 µM Cd			5 µM Cd	
WT	***cad1–3***		**WT**	***cad2***
303.9 ± 8.3	79.2 ± 3.2*	Leaf [Cd] (mg/g DW)	**756±37**	304±57*
398±24	**835±32***	Root [Cd] (mg/g DW)	847±199	**2249±120***
0.77±0.03	0.096±0.008*	Cd TF	**1.03±0.30**	0.14±0.03*

Values represent the average ± SE of at least three biological replicates. Statistically significant differences between each Cd-exposed mutant and its corresponding WT were shown using asterisks (*), with the highest value highlighted in bold (two-sample *t*-test, $p < 0.05$). DW: dry weight, TF: translocation factor.

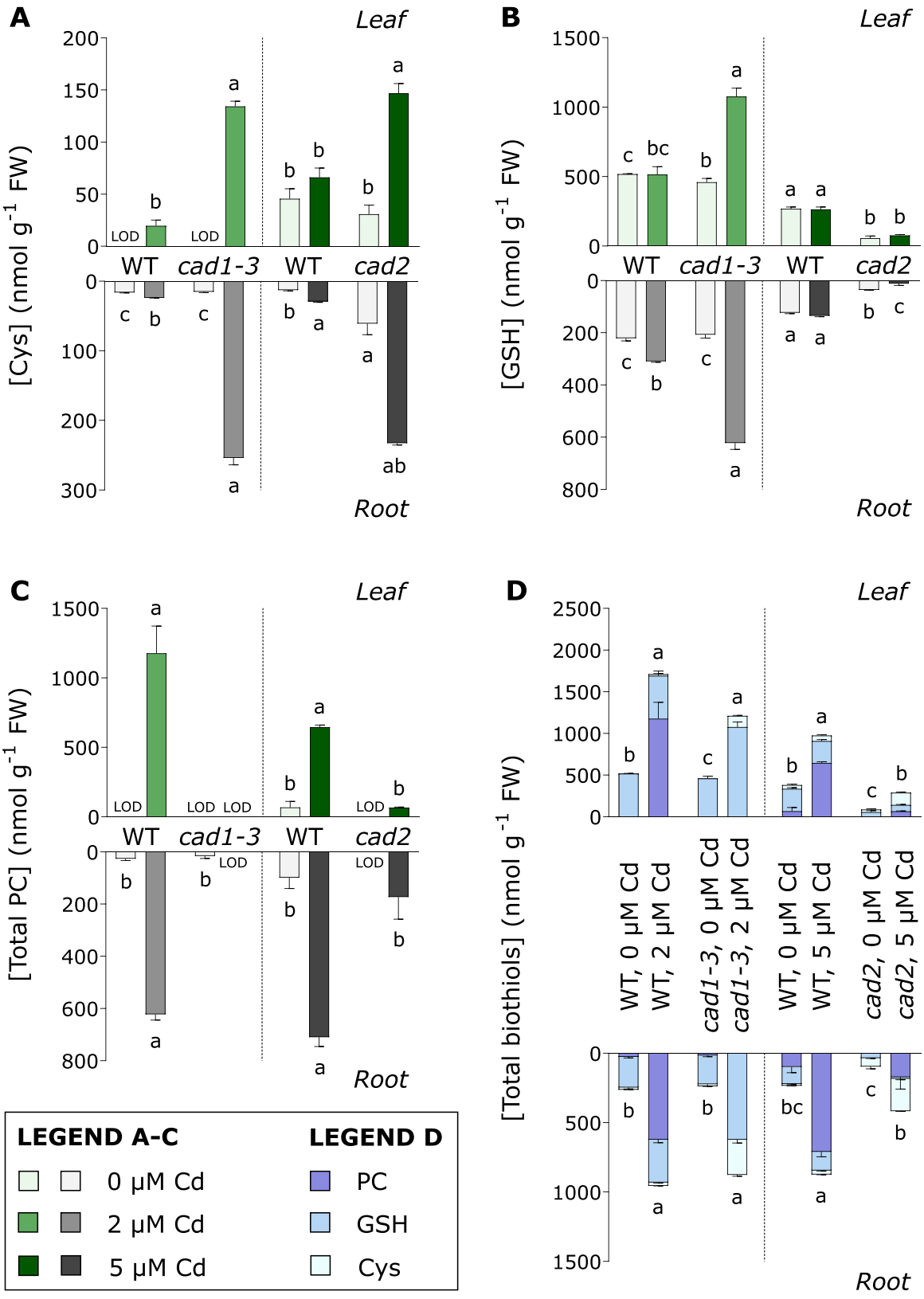

Fig. 3. **(A)** Cysteine, **(B)** glutathione, **(C)** total phytochelatin and **(D)** total biothiol concentrations (nmol g^{-1} FW) in leaves and roots of hydroponically grown, three-week-old wild-type (WT) as well as cadmium (Cd)-sensitive *cad1-3* and *cad2* mutant *Arabidopsis thaliana* plants after exposure to 0, 2 or 5 µM $CdSO_4$ for 24 h. Values represent the average + SE of at least three biological replicates. Statistically significant differences between each mutant and its corresponding WT per organ are shown using different letters (parametric two-way ANOVA with post-hoc Tukey HSD test or non-parametric Kruskal-Wallis rank sum test with post-hoc Wilcoxon rank sum test, $p < 0.05$). Cys: cysteine, FW: fresh weight, GSH: glutathione, LOD: limit of detection, PC: phytochelatin.

Table 2
Cadmium (Cd)-induced fold changes of normalised oxidative stress hallmark transcript levels in leaves and roots of three-week-old, hydroponically grown wild-type (WT) as well as Cd-sensitive *cad1-3* and *cad2* mutant *Arabidopsis thaliana* plants after exposure to 2 or 5 μM $CdSO_4$ for 24 h.

2 μM Cd							Gene	5 μM Cd						
WT			*cad1-3*					WT			*cad2*			
Leaf														
13.90	±	0.66	4.46	±	0.26		*AT1G57630*	26.9	±	1.7	26.0	±	1.8	
5.50	±	0.68	7.33	±	0.40		*CYSTM1*	**20.0**	**±**	**3.6**	8.1	±	1.2	*
13.5	±	1.8	17.58	±	0.55		*HUP35*	25.7	±	2.1	42.7	±	2.9	
4.69	±	0.24	**91**	**±**	**15**	*	*TI1*	10.7	±	1.0	15.1	±	1.9	
0.97	±	0.08	**27.0**	**±**	**2.5**	*	*UPOX*	4.76	±	0.35	**7.30**	**±**	**0.78**	*
Root														
3.01	±	0.12	**106.9**	**±**	**5.3**	*	*AT1G57630*	2.83	±	0.25	**20.4**	**±**	**2.7**	*
0.93	±	0.09	**3.41**	**±**	**0.29**	*	*CYSTM1*	0.95	±	0.13	1.20	±	0.10	
8.13	±	0.39	**70.7**	**±**	**1.5**	*	*HUP35*	10.2	±	1.8	**32.8**	**±**	**6.2**	*
0.97	±	0.21	**509**	**±**	**64**	*	*TI1*	25.5	±	4.6	15.4	±	1.8	
0.90	±	0.07	**6.80**	**±**	**0.28**	*	*UPOX*	1.354	±	0.064	**2.76**	**±**	**0.51**	*

Normalised gene expression levels following Cd stress were set relative to the control condition (0 μM $CdSO_4$) of each genotype to calculate Cd-induced fold changes. These Cd-induced fold changes are depicted as the average ± SE of at least three biological replicates. Statistically significant differences were determined for each Cd-sensitive mutant (*cad1-3* or *cad2*) compared to its corresponding WT using the parametric two-way ANOVA with post-hoc Tukey HSD test ($p < 0.05$). A green ▢ colour indicates a significant Cd-induced upregulation of a gene within one genotype compared to the untreated control, while an asterisk (*) denotes whether the Cd-induced fold changes of the mutant and corresponding WT are different. In this case, the highest value is indicated in bold. *AT1G57630: toll-interleukin-resistance (TIR) domain family protein, CYSTM1: cysteine-rich transmembrane module 1, HUP35: hypoxia response unknown protein 35, TI1: trypsin inhibitor protein 1, UPOX: upregulated by oxidative stress.*

which were elevated to a larger extent compared to the WT plants upon Cd exposure (Fig. 3A-B).

Besides affecting levels of these biothiols, Cd exposure also induced the expression of several oxidative stress hallmark genes in leaves and roots of all genotypes after 24 h (Table 2). In accordance with a concentration-dependent effect of Cd, more transcripts were upregulated in WT plants after exposure to 5 μM Cd compared to 2 μM Cd. While the number of upregulated genes was rather similar between the *cad2* mutant and the WT after treatment with 5 μM Cd, more genes were upregulated in the *cad1-3* mutant compared to the WT after exposure to 2 μM Cd. Furthermore, the observed Cd-induced upregulations of several of these genes were larger in both Cd-sensitive mutants than in their WT counterparts (Table 2), pointing towards more severe oxidative stress in these mutants. This effect was most pronounced in the *cad1-3* mutant and especially evident at the root level. Although most observations pointed towards a larger oxidative challenge in the *cad* mutants, two genes showed the opposite pattern [*AT1G57630* in *cad1-3* (trend, $p = 0.051$) and *CYSTM1* in *cad2*] (Table 2). Notably, the mutants showed an altered expression of at least one oxidative stress hallmark gene compared to their WT under control conditions (Supplemental Table S3), suggesting that their basal oxidative stress level already differed from that of WT plants.

3.3. Cadmium induces endoplasmic reticulum stress with transcript levels of inositol requiring 1-dependent decay of mRNA targets decreasing during higher stress intensities

Changes in the oxidative environment are known to be intertwined with ER stress (Depaepe et al., 2021; Cao et al., 2022). Therefore, to gain insight into the ER-UPR in the Cd stress intensity framework of the current study, the expression levels of *bZIP60s* and three target genes regulated (partly) by bZIP60 under ER stress [(*BiP3, ERO1, TIN1*) (Iwata et al., 2008)] were determined. In addition, the expression of unspliced *bZIP60* (*bZIP60us*) was determined, as it was previously shown that the induction of *bZIP60s* over *bZIP60us* by metal exposure in *A. thaliana* depends on the studied metal and its applied concentration (Demircan et al., 2024). A concentration-dependent stimulation of the ER-UPR in roots of WT plants was evident, as 2 μM Cd only significantly induced the expression of *BiP3*, while 5 μM Cd elevated transcript levels of the three investigated target genes (Table 3). Nevertheless, the lack of significant upregulations of *bZIP60s* or *bZIP60us* and the lack of an increased ratio between both in Cd-exposed WT roots suggests that increased *bZIP60* splicing either preceded the induction of these target genes or that other master regulators of the ER stress response were involved (Table 3; Supplemental Figure S2). In contrast to roots, leaves of WT plants already showed a significant induction of all investigated genes as well as the ratio between *bZIP60s* and *bZIP60us* after exposure to only 2 μM Cd, which remained after exposure to the higher Cd concentration (Table 3; Supplemental Figure S2). This points towards a different stimulation of the ER-UPR, and plausibly, a different extent of ER stress in leaves and roots following Cd exposure, with leaves being seemingly more sensitive to this type of stress than roots. When Cd stress intensity was increased by using the *cad* mutants, the ratio between *bZIP60s* and *bZIP60us* significantly increased in mutant roots, which also showed larger Cd-induced upregulations of all ER-UPR genes than their WT counterparts (Table 3; Supplemental Figure S2). Conversely, Cd-induced fold changes of these genes were generally less pronounced or similar in mutant leaves compared to WT leaves (Table 3), with the ratio between *bZIP60s* and *bZIP60us* also increasing to a similar degree between both genotypes (Supplemental Figure S2).

In addition to genes related to the ER-UPR, expression levels of *interactor of synaptotagmin 1* (*ROSY1*) and a pathogenesis-related (PR)-14 family gene (*AT5G01870*) were determined. These two transcripts were reported to be among the most vulnerable RIDD targets, and they

Table 3
Cadmium (Cd)-induced fold changes of normalised endoplasmic reticulum (ER) stress-related transcript levels in leaves and roots of three-week-old, hydroponically grown wild-type (WT) as well as Cd-sensitive *cad1-3* and *cad2* mutant *Arabidopsis thaliana* plants after exposure to 2 or 5 μM $CdSO_4$ for 24 h.

2 μM Cd							Gene	5 μM Cd						
WT			*cad1-3*					WT			*cad2*			
Leaf														
2.27	±	0.21	**8.03**	±	**0.74**	*	*bZIP60us*	5.69	±	0.25	5.70	±	0.12	
7.86	±	0.66	**21.0**	±	**4.7**	*	*bZIP60s*	13.9	±	1.1	12.57	±	0.42	
15.4	±	**2.6**	1.38	±	0.20	*	*BiP3*	**27.74**	±	**0.55**	7.16	±	0.41	*
6.8	±	**1.2**	2.05	±	0.20	*	*ERO1*	**9.68**	±	**0.21**	3.74	±	0.13	*
6.9	±	1.1	4.67	±	0.31		*TIN1*	10.39	±	0.46	11.76	±	0.52	
0.63	±	**0.33**	0.010	±	0.003	*	*AT5G01870*	1.08	±	0.11	1.06	±	0.04	
0.44	±	0.08	0.06	±	0.02		*ROSY1*	ND			0.22	±	0.13	
Root														
0.86	±	0.17	**8.2**	±	**1.8**	*	*bZIP60us*	1.27	±	0.10	**3.18**	±	**0.30**	*
1.59	±	0.23	**238.6**	±	**6.9**	*	*bZIP60s*	1.29	±	0.26	**40.2**	±	**6.5**	*
11.1	±	4.4	**312**	±	**12**	*	*BiP3*	14.2	±	2.6	**650**	±	**51**	*
1.37	±	0.08	**3.04**	±	**0.21**	*	*ERO1*	2.44	±	0.31	**3.98**	±	**0.47**	*
1.27	±	0.17	**46.0**	±	**2.1**	*	*TIN1*	2.64	±	0.42	**40.9**	±	**4.2**	*
1.07	±	**0.13**	0.010	±	0.003	*	*AT5G01870*	0.77	±	0.06	1.05	±	0.18	
1.30	±	**0.59**	0.011	±	0.004	*	*ROSY1*	0.16	±	0.03	0.11	±	0.01	

Normalised gene expression levels following Cd stress were set relative to the control condition (0 μM $CdSO_4$) of each genotype to calculate Cd-induced fold changes. These Cd-induced fold changes are depicted as the average ± SE of at least three biological replicates. Statistically significant differences were determined for each Cd-sensitive mutant (*cad1-3* or *cad2*) compared to its corresponding WT using the parametric two-way ANOVA with post-hoc Tukey HSD test ($p < 0.05$). A green or red colour respectively indicates a significant Cd-induced up- or downregulation of a gene within one genotype compared to the untreated control, while an asterisk (*) denotes whether the Cd-induced fold changes of the mutant and corresponding WT are different. In this case, the highest value is indicated in bold. ND: not detected (i.e. did not reach threshold within 60 cycles). *AT5G01870: pathogenesis-related (PR) protein belonging to the PR-14 family, BiP3: binding protein 3, bZIP60: basic region/leucine zipper motif 60, bZIP60s:* spliced *bZIP60, bZIP60us:* unspliced *bZIP60, ERO1: ER oxidoreductin 1, IRE1: inositol requiring 1, ROSY1: interactor of synaptotagmin 1, TIN1: tunicamycin induced 1.*

encode inhibitors of autophagy (Bao et al., 2018). Lower *ROSY1* levels were observed in WT and *cad2* mutant roots and leaves (trend for *cad2* mutant leaves, $p = 0.069$) after exposure to 5 μM Cd (Table 3). As such, this indicates that the downregulation of this transcript is most relevant from moderate Cd stress onwards, pointing towards a dependence on Cd stress intensity. This was supported by the finding that *ROSY1* and *AT5G01870* transcript levels were unaltered in WT plants but decreased in more severely-stressed *cad1-3* mutant plants after exposure to 2 μM Cd. As the *cad1-3* mutant is the only genotype that showed a significant Cd-induced downregulation of *AT5G01870* (Table 3), this further supports that a complete lack of PC induction, despite GSH accumulation, most severely affects the Cd stress response.

It should be mentioned that the stronger ER stress response in Cd-exposed *cad* mutant roots than in WT roots could be attributed to their higher Cd retention (Table 1; Table 3). While the lower Cd concentrations in Cd-exposed *cad* mutant leaves than in WT leaves are also in accordance with their weaker inductions of *BiP3* and *ERO1*, they are in contrast with their similar or larger downregulations of *ROSY1* (Table 1; Table 3). Notably, a downregulation of *ROSY1* also appears connected to RIDD during Cd stress, as a decreased level of this transcript was observed in leaves of WT, but not in *ire1* double mutant, plants following moderate Cd stress (Supplemental Figure S3B). As such, our results suggest that the type of ER stress response in leaves shifts in a Cd stress intensity-dependent manner, with the stimulation of RIDD (at least of *ROSY1*) predominating over that of the ER-UPR when Cd stress intensity increases.

3.4. Cadmium-induced autophagy is stimulated upon higher stress intensity and correlates with the transcript levels of inositol requiring 1-dependent decay of mRNA targets

As *ROSY1* and *AT5G01870*, of which transcript levels decreased in response to Cd exposure (Table 3), were previously found to inhibit autophagy (Bao et al., 2018), this process was examined next. A clear Cd concentration-dependent stimulation of *ATG* gene expression and the degree of ATG8 lipidation (i.e. ATG8-PE/total ATG8) was observed for WT plants (Fig. 4; Table 4). More specifically, only a few *ATG* genes were induced after exposure to 2 μM Cd, while almost all investigated genes showed higher expression levels after exposure to 5 μM Cd (Table 4). In accordance with *ATG8* upregulation being strongly induced, the

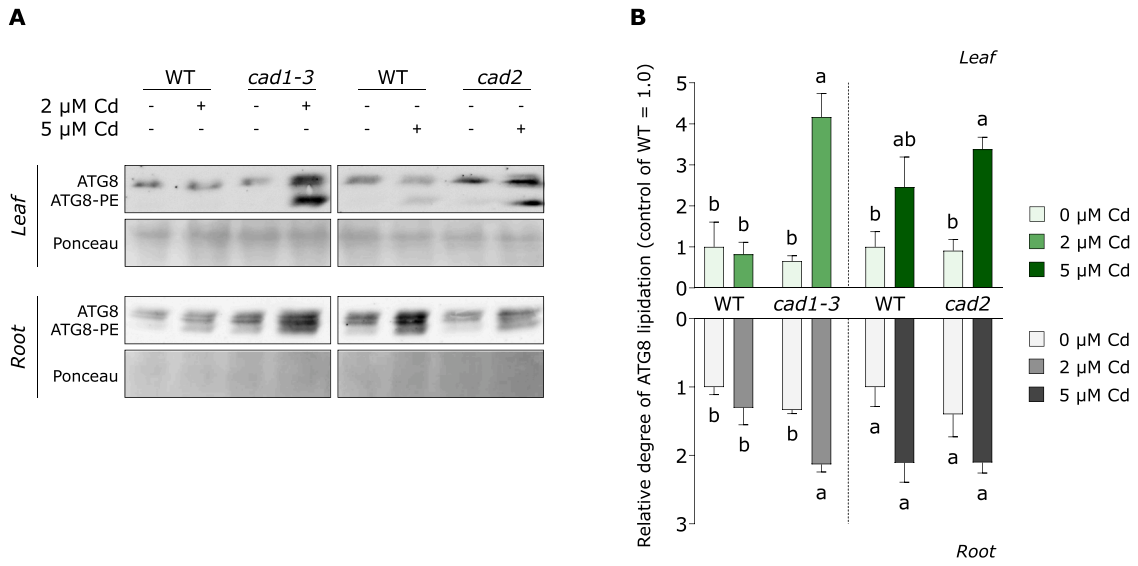

Fig. 4. **(A)** Immunoblot showing soluble and lipidated (phosphatidylethanolamine (PE)-conjugated) autophagy-related 8 (ATG8) abundance in leaves and roots of three-week-old, hydroponically grown wild-type (WT) as well as cadmium (Cd)-sensitive *cad1-3* and *cad2* mutant *Arabidopsis thaliana* plants exposed to 0, 2 or 5 µM $CdSO_4$ for 24 h. Total proteins are visualised using Ponceau S staining. **(B)** The degree of ATG8 lipidation (i.e. ATG8-PE/total ATG8) was quantified from immunoblots and expressed relative to the control (0 µM $CdSO_4$) of each WT. Values represent the average + SE of three biological replicates. Significant differences between each mutant and its corresponding WT per organ are signified using different letters (parametric two-way ANOVA with post-hoc Tukey HSD test, $p < 0.05$). An asterisk (*) indicates a trend towards a significant difference between a condition and the control condition of the corresponding WT ($p < 0.08$).

abundances of ATG8-PE were visibly higher in both leaves and roots after exposure to 5 µM Cd (Fig. 4A), which also led to increasing trends for the degree of ATG8 lipidation (Fig. 4B). To further confirm autophagy stimulation following acute Cd stress, autophagic structures were visualised in roots of a GFP-ATG8H reporter line additionally treated with 0.5 µM concanamycin A for 2 h before confocal imaging. This V-ATPase inhibitor enables autophagic structure visualisation in plants by limiting autophagic body degradation, which was expected to relate to its effect on vacuolar pH (Yoshimoto et al., 2004). Quantification of GFP-ATG8H puncta in trichoblasts with early root hair formation showed that they were indeed significantly more abundant in Cd-treated plants compared to control plants (Supplemental Figure S4A). This Cd-mediated increase in GFP-ATG8H puncta was largely lost when omitting concanamycin A treatment prior to imaging, indicating that Cd exposure did not significantly inhibit autophagic body degradation (Supplemental Figure S4B). Additionally, exposure of the GFP-ATG8H reporter plants to various Cd concentrations for six days confirmed that their Cd sensitivity is still similar to that of WT plants (Supplemental Figure S5).

In addition, immunoblot results showed an induction of both soluble and lipidated ATG8 in leaves and roots of WT plants and in *cad2* mutant roots after exposure to 5 µM Cd (Fig. 4A). Accordingly and in agreement with the similarly decreased *ROSY1* transcript levels in both Cd-exposed genotypes (Table 3), ATG8 lipidation degrees were also similar between Cd-exposed WT and *cad2* mutant plants (Fig. 4B), despite the relatively low levels of GSH in this mutant (Fig. 3B). In contrast, the Cd-induced fold changes of several *ATG8* transcript levels were still different for both genotypes (Table 4). These differences were ambiguous in the roots of *cad2* mutant plants, as both less and more pronounced Cd-mediated inductions were observed in comparison to their WT counterparts, suggesting that the significance of the *ATG8* genes during Cd stress may shift between both genotypes. In contrast, leaves of *cad2* mutant plants showed weaker Cd-induced upregulations for almost all *ATG8* genes compared to WT counterparts (Table 4), suggesting that there might be a limit to autophagy induction in this mutant genotype. This could be related to higher expression levels of these genes in *cad2* mutant leaves than in WT leaves under control conditions (Supplemental Table S3).

Even though transcript data for the *cad2* mutant leaves suggest that *ATG* upregulation is limited upon an increased Cd stress response, the *cad1–3* did show more pronounced upregulations of almost all *ATG* genes in both leaves and roots than the WT (Table 4). In contrast to the *cad2* mutant, transcript levels of the *ATG* genes were mostly similar between WT and *cad1-3* mutant plants under control conditions (Supplemental Table S3), corroborating that this altered basal expression of many *ATG8* genes in the *cad2* mutant may indeed have contributed to a lower demand or capacity to further increase *ATG8* expression (Table 4). Furthermore, both soluble and lipidated ATG8 abundances were increased in *cad1-3* mutant plants after exposure to only 2 µM Cd in both leaves and roots (Fig. 4A). Consistent with severe Cd-induced decreases in *AT5G01870* and *ROSY1* transcript levels in the *cad1-3* mutant, higher ATG8 lipidation degrees were observed in this Cd-exposed mutant compared to both the mutant under control conditions and the corresponding Cd-exposed WT (Fig. 4B). These results support an intensity-dependent effect of Cd stress on autophagy stimulation that cannot be alleviated by accumulating high levels of GSH (Fig. 3B).

Lastly, data from our experimental set-up showed that the geometric mean of the normalised expression of *AT5G01870* and *ROSY1* was negatively correlated with the geometric mean of the normalised expression of *ATG8* genes (Fig. 5A). Furthermore, this first parameter, which was based on gene expression data, even showed a strong trend towards a negative correlation to the degree of ATG8 lipidation, which was based on the immunoblots (Fig. 5B). Notably, leaves were especially prone to ER stress and appeared to shift their stimulation of the ER-UPR to RIDD (at least of *ROSY1*) upon more intense Cd stress (Table 3), which was observed concomitantly with Cd-mediated increases in the degree of ATG8 lipidation that were larger in leaves than in roots (Fig. 4B). In agreement with *ROSY1* transcript levels decreasing IRE1-dependently following moderate Cd stress, Cd-induced *ATG8H* induction was abrogated in leaves of the *ire1* double mutant (Supplemental Figure S3), further corroborating that Cd-induced ER stress and autophagy appear connected in leaves.

3.5. *The acute cadmium-induced ethylene response is enhanced with increasing stress intensity*

The phytohormone ethylene is an important mediator of the acute Cd

Table 4
Cadmium (Cd)-induced fold changes of normalised *autophagy-related* (*ATG*) transcript levels in leaves and roots of three-week-old, hydroponically grown wild-type (WT) as well as Cd-sensitive *cad1-3* and *cad2* mutant *Arabidopsis thaliana* plants after exposure to 2 or 5 μM $CdSO_4$ for 24 h.

2 μM Cd							Gene	5 μM Cd						
WT			*cad1-3*					WT			*cad2*			
Leaf														
1.97	±	0.12	**4.82**	±	**0.27**	*	*ATG8A*	**6.80**	±	**0.53**	1.92	±	0.20	*
1.50	±	0.18	**3.84**	±	**0.25**	*	*ATG8B*	**7.36**	±	**0.68**	3.10	±	0.31	*
1.34	±	0.17	1.43	±	0.05		*ATG8C*	1.66	±	0.19	1.23	±	0.07	
1.38	±	0.17	**2.93**	±	**0.09**	*	*ATG8D*	**3.28**	±	**0.22**	1.33	±	0.14	*
1.50	±	0.21	**8.99**	±	**0.59**	*	*ATG8E*	**11.02**	±	**0.49**	3.56	±	0.75	*
1.02	±	0.06	**1.67**	±	**0.09**	*	*ATG8F*	1.95	±	0.34	1.88	±	0.17	
1.22	±	0.10	1.60	±	0.04		*ATG8G*	**2.73**	±	**0.24**	1.68	±	0.13	*
1.58	±	0.26	**8.99**	±	**0.20**	*	*ATG8H*	**11.35**	±	**0.61**	4.42	±	0.73	*
1.70	±	0.17	**2.98**	±	**0.20**	*	*ATG8I*	**3.64**	±	**0.48**	1.78	±	0.23	*
1.64	±	0.20	**7.70**	±	**0.35**	*	*ATG18A*	2.99	±	0.16	**5.18**	±	**0.46**	*
Root														
1.46	±	0.13	**4.32**	±	**0.10**	*	*ATG8A*	1.631	±	0.075	**1.96**	±	**0.09**	*
1.27	±	0.05	**3.93**	±	**0.45**	*	*ATG8B*	2.89	±	0.28	3.02	±	0.12	
1.24	±	0.10	1.287	±	0.076		*ATG8C*	**1.19**	±	**0.07**	0.69	±	0.04	*
1.21	±	0.09	**3.17**	±	**0.17**	*	*ATG8D*	**2.46**	±	**0.10**	1.88	±	0.09	*
1.36	±	0.20	**22.4**	±	**1.9**	*	*ATG8E*	2.59	±	0.14	**5.98**	±	**0.36**	*
1.23	±	0.19	**4.93**	±	**0.28**	*	*ATG8F*	**1.43**	±	**0.06**	0.881	±	0.007	*
1.36	±	0.07	**2.24**	±	**0.12**	*	*ATG8G*	1.56	±	0.08	1.43	±	0.08	
0.90	±	0.06	**15.5**	±	**1.3**	*	*ATG8H*	4.09	±	0.27	4.42	±	0.21	
1.21	±	0.09	**3.02**	±	**0.14**	*	*ATG8I*	1.67	±	0.01	1.60	±	0.05	
1.68	±	0.14	**7.55**	±	**0.85**	*	*ATG18A*	1.90	±	0.06	**4.42**	±	**0.13**	*

Normalised gene expression levels following Cd stress were set relative to the control condition (0 μM $CdSO_4$) of each genotype to calculate Cd-induced fold changes. These Cd-induced fold changes are depicted as the average ± SE of at least three biological replicates. Statistically significant differences were determined for each Cd-sensitive mutant (*cad1-3* or *cad2*) compared to its corresponding WT using a parametric two-way ANOVA with post-hoc Tukey HSD test ($p < 0.05$). A green or red colour respectively indicates a significant Cd-induced up- or downregulation of a gene within one genotype compared to the untreated control, while an asterisk (*) denotes whether the Cd-induced fold changes of the mutant and corresponding WT are different. In this case, the highest value is indicated in bold.

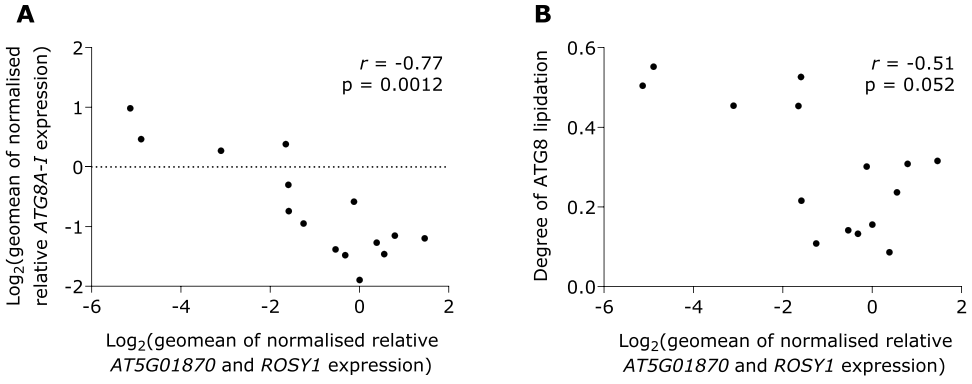

Fig. 5. Spearman's correlations (*r*) between the geometric mean (geomean) of the normalised transcript levels of *AT5G01870* and *ROSY1* (x-axis) and **(A)** the geometric mean of the normalised transcript levels of *ATG8A-1* (y-axis) or **(B)** the degree of ATG8 lipidation (i.e. lipidated/total ATG8) (y-axis). Data were obtained from three-week-old, hydroponically grown wild-type (WT), *cad1-3* and *cad2* mutant *Arabidopsis thaliana* leaves and roots after exposure to 0, 2 or 5 μM $CdSO_4$ for 24 h. To correlate different parameters, averages of each condition (genotype, Cd exposure, organ) were used as input data. Gene expression data were $\log_2$-transformed. *AT5G01870: pathogenesis-related (PR) protein belonging to the PR-14 family, ATG8: autophagy-related 8, ROSY1: interactor of synaptotagmin 1.*

stress response (Schellingen et al., 2015) and was suggested to be related to autophagy and, potentially, the ER stress response (Depaepe et al., 2021). Therefore, ethylene emission was determined and linked to transcriptional changes in its downstream signalling response and the biosynthesis of its precursor 1-aminocyclopropane-1-carboxylic acid (ACC) in the Cd stress response of varying intensities. As ethylene accumulation over a time period of 24 h was measured in glass cuvettes connected to a photoacoustic detection system, plants were grown on rockwool plugs that could easily be transferred to this cuvette system. To achieve similar leaf Cd concentrations as in the hydroponic cultivation system, a Cd concentration of 25 μM was used (Supplemental Figure S6). Results showed that ethylene production increased in the Cd-sensitive mutants but not in WT plants after exposure to 25 μM Cd (Fig. 6). The Cd-exposed *cad1-3* mutant showed the largest ethylene production, which was approximately three times higher than that of Cd-exposed *cad2* plants (Fig. 6). As such, these results support that Cd-induced ethylene emission is increasingly stimulated upon higher Cd stress intensity. While 25 μM Cd did not affect ethylene emission in WT plants after 24 h (Fig. 6), higher concentrations of Cd did increase this parameter in a concentration-dependent manner (Supplemental Figure S7).

In addition, the expression of *WRKY DNA-binding factor 33* (*WRKY33*), which positively regulates *ACS2* expression (Li et al., 2012), and genes related to the biosynthesis and signalling of ethylene were largely induced in leaves and roots of WT plants exposed to both 2 and 5 μM Cd for 24 h (Table 5). Although leaves of the *cad2* mutant plants showed largely similar responses as those of WT plants after exposure to 5 μM Cd, roots of this mutant showed larger Cd-induced upregulations than their WT counterparts. For the *cad1-3* mutant plants, more pronounced Cd-mediated inductions for most of these genes were not only observed in roots, but also in leaves (Table 5). This generally corroborates higher ethylene biosynthesis and signalling with increasing Cd stress. The expression of these genes was similar between the Cd-sensitive mutants and their corresponding WT plants after growth under control conditions (Supplemental Table S3).

3.6. More severe cadmium stress increasingly shunts the ethylene precursor 1-aminocyclopropane-1-carboxylic acid to conjugation

To gain insight into the stimulation of the ethylene biosynthesis pathway at the metabolic level in WT, *cad1-3* and *cad2* mutant plants, the concentrations of free ACC were determined in roots and leaves of these genotypes upon Cd exposure and set relative to those of the corresponding unexposed WT. In addition, the relative quantity of malonyl-ACC (MACC) was also determined to gain insight into the extent of ACC conjugation upon increasing Cd stress.

Free ACC and MACC levels were affected concentration- and organ-dependently, with only leaves showing significant Cd-induced increases (Fig. 7). As for ethylene-related gene expression and ethylene production (Fig. 6; Supplemental Table S3), ACC and MACC levels of mutant plants were similar to those of WT plants under control conditions (Fig. 7). Nevertheless, with the exception of free ACC levels in Cd-exposed *cad2* mutant leaves, these parameters were also affected to a higher degree in the Cd-sensitive mutants after Cd exposure (Fig. 7), further corroborating the stress-dependent effect of Cd on the ethylene biosynthesis pathway. Furthermore, this indicates that relatively high free ACC levels are mostly observed concomitantly with relatively high MACC levels. One exception, however, is that leaves of the Cd-exposed *cad2* mutant showed a less pronounced increase in free ACC but a larger increase in MACC levels compared to their WT counterparts (Fig. 7), suggesting that its larger extent of conjugation limited the increase in free ACC levels.

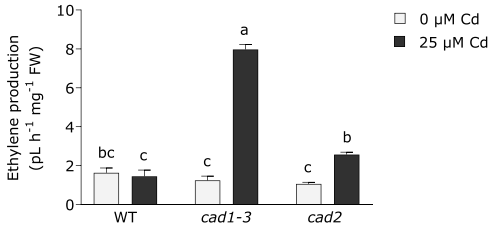

Fig. 6. Ethylene production (pL h^{-1} mg^{-1} FW) in wild-type (WT) as well as cadmium (Cd)-sensitive *cad1-3* and *cad2* mutant plants grown on rockwool for three weeks under control conditions and exposed to 0 or 25 μM $CdSO_4$ for 24 h. Data represent the average + SE of three biological replicates. Different letters depict statistically significant differences (two-way ANOVA with post-hoc Tukey HSD test, $p < 0.05$). FW: fresh weight.

4. Discussion

4.1. An exploration of the cadmium stress intensity framework using different cadmium concentrations and cadmium-sensitive mutant plants

The aim of this research was to gain insight into the acute Cd stress response of differing short-term stress intensities. Therefore, three-week-old, hydroponically grown WT *A. thaliana* plants were exposed to 2 μM or 5 μM Cd at the root level for 24 h to respectively induce a mild or moderate acute stress response that will, for the sake of simplicity, frequently be referred to as such. Data verified that increasing the Cd concentration from 2 μM to 5 μM Cd significantly induced a stronger stress response in WT plants, based on the concentration-dependent effect that was observed for long-term rosette diameter expansion and the acute upregulation of oxidative stress hallmark genes (Fig. 1D; Table 2). Next to the increasing oxidative stress response caused by Cd exposure, the accumulation of the biothiols cysteine, GSH and PC was also evident. As PCs are well-known to be involved in metal detoxification (Seregin and Kozhevnikova, 2023), their pronounced increase likely contributed to limiting the severity of the Cd stress response. Although the two experiments were not statistically compared, it should be noted that PC levels of plants exposed to moderate Cd stress were in a similar range as those of plants exposed to mild Cd stress (Fig. 3C). Accordingly, similar total PC production was also observed in *A. thaliana* leaves and roots after 24 h exposure to 5 and 10 μM Cd (Jozefczak et al., 2014), and PC concentrations were also found not to increase further when *A. thaliana* cells were exposed to 400 μM instead of 200 μM Cd for 24 h (Ducruix et al., 2006). This suggests that there is a limit to the degree of early PC production, potentially related to the availability of GSH that is depleted early after Cd exposure and needs to be replenished (Jozefczak et al., 2014; Deckers et al., 2020). Although root PC levels were not significantly different, more time was indeed required before GSH levels of *A. thaliana* recovered from their initial depletion following exposure to 10 μM compared to 5 μM Cd (Jozefczak et al., 2014). As such, this might determine the extent of early Cd detoxification and hence the cellular stress response (Fig. 8). Nevertheless, even *A. thaliana* plants exposed to 5 (or 10) μM Cd produce viable progeny (Keunen et al., 2011).

Next to altering Cd concentrations to vary stress intensity, Cd-sensitive mutant *A. thaliana* plants (*cad1-3* and *cad2*) were studied. The *cad1-3* and *cad2* mutants are known for their heightened Cd sensitivity due to a lack of PC production (Howden et al., 1995b) or decreased GSH and PC levels (Howden et al., 1995a), respectively, as was also confirmed in the current study (Figs. 1–3; Table 2). In contrast to the *cad2* mutant (Hendrix et al., 2020), the *cad1-3* mutant was unable to produce viable seeds following long-term exposure to 5 μM Cd (Iven, unpublished results). Furthermore, as this mutant already halted its rosette diameter increase in response to 2 μM Cd exposure for one week (Fig. 1D), the exposure of this mutant was limited to this Cd concentration within our experimental set-up.. On the other hand, the *cad2* mutant was then employed and exposed to the higher Cd concentration in our framework (i.e. 5 μM Cd) to still induce more severe Cd stress than for WT plants exposed to this Cd concentration without exacerbating Cd

Table 5
Cadmium (Cd)-induced fold changes of normalised ethylene-related transcript levels in leaves and roots of three-week-old, hydroponically grown wild-type (WT) as well as Cd-sensitive *cad1–3* and *cad2* mutant *Arabidopsis thaliana* plants after exposure to 2 or 5 μM $CdSO_4$ for 24 h.

2 μM Cd							Gene	5 μM Cd						
WT			*cad1-3*					WT			*cad2*			
Leaf														
3.04	±	0.83	**13.15**	±	**0.89**	*	*WRKY33*	11.94	±	0.89	9.56	±	0.79	
40	±	13	**514**	±	**32**	*	*ACS2*	50.3	±	7.7	91	±	20	
1.28	±	0.10	**8.24**	±	**0.64**	*	*ACO2*	3.57	±	0.22	**5.85**	±	**0.54**	*
37.4	±	7.1	50.7	±	7.8		*ERF1*	143.7	±	8.8	116	±	10	
Root														
1.65	±	0.11	**17.2**	±	**1.5**	*	*WRKY33*	4.03	±	0.54	**14.7**	±	**1.6**	*
1.03	±	0.24	**109.8**	±	**3.5**	*	*ACS2*	0.803	±	0.038	**47**	±	**12**	*
2.95	±	0.22	3.32	±	0.02		*ACO2*	2.71	±	0.23	**4.24**	±	**0.41**	*
22.2	±	3.0	**95.7**	±	**4.4**	*	*ERF1*	56	±	16	**136**	±	**20**	*

Normalised gene expression levels following Cd stress were set relative to the control condition (0 μM $CdSO_4$) of each genotype to calculate Cd-induced fold changes. These Cd-induced fold changes are depicted as the average ± SE of at least three biological replicates. Statistically significant differences were determined for each Cd-sensitive mutant (*cad1-3* or *cad2*) compared to its corresponding WT using a parametric two-way ANOVA with post-hoc Tukey HSD test ($p < 0.05$). A green colour indicates a significant Cd-induced upregulation of a gene within one genotype compared to the untreated control, while an asterisk (*) denotes whether the Cd-induced fold changes of the mutant and corresponding WT are different. In this case, the highest value is indicated in bold. *ACS2: 1-amino-cyclopropane-1-carboxylic acid (ACC) synthase 2, ACO2: ACC oxidase 2, ERF1: ethylene response factor 1, WRKY33: WRKY DNA-binding protein 33.*

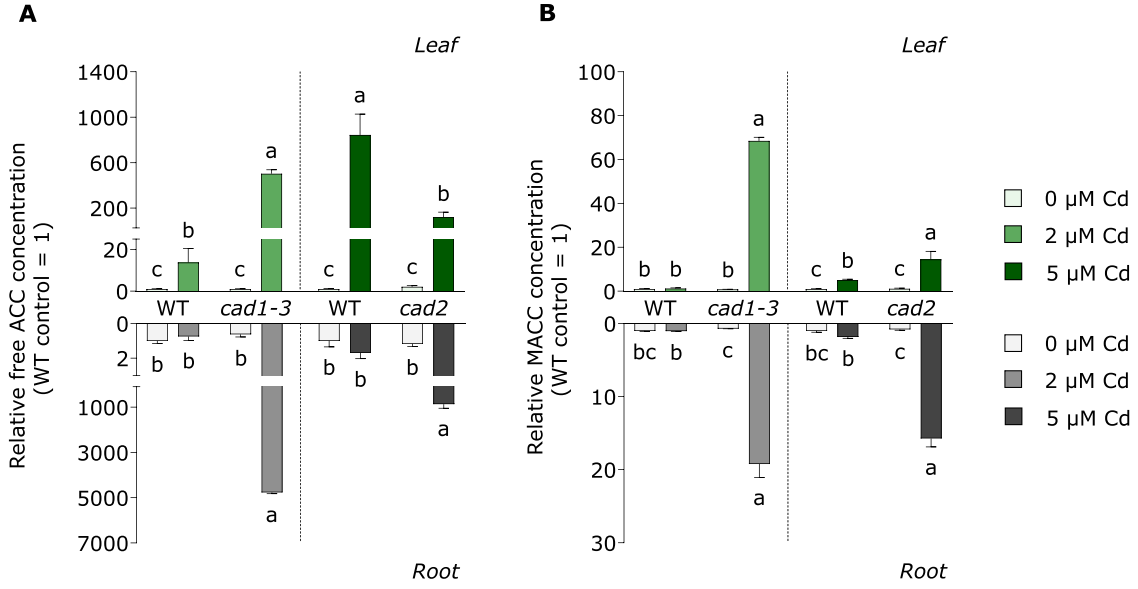

Fig. 7. (A) Relative free 1-aminocyclopropane-1-carboxylic acid (ACC) and **(B)** relative malonyl-ACC (MACC) concentrations in three-week-old, hydroponically grown wild-type (WT) as well as cadmium (Cd)-sensitive *cad1-3* and *cad2* mutant *Arabidopsis thaliana* plants exposed to 0, 2 or 5 μM $CdSO_4$ for 24 h. Data, expressed relative to the control condition (0 μM $CdSO_4$) of each WT, represent the average + SE for at least four biological replicates. Different letters are used to depict statistically significant differences between each mutant and its corresponding WT per organ (two-way ANOVA with post-hoc Tukey HSD test or non-parametric Kruskal-Wallis rank sum test with post-hoc Wilcoxon rank sum test, $p < 0.05$).

toxicity (Fig. 1; Fig. 2). Regarding the stress intensity framework, it should be noted that the more intense acute Cd stress response in *cad* mutants compared to the WT was especially evident at the root level (Fig. 2A; Table 2), bearing the highest Cd concentrations (Table 1). Consistent with PCS1 contributing to root-to-shoot translocation of Cd in *Triticum aestivum* (Gong et al., 2003), lower root-to-leaf Cd translocation factors were observed in *cad1–3* and *cad2* mutants [Table 1, (Gielen et al., 2017; Deckers et al., 2021)]. While one could hence argue that stress intensity in these mutants was determined by their higher Cd retention in roots, this would be insufficient to explain the findings of the current study. For instance, *cad1-3* mutants exhibited a reduced root fresh weight after exposure to 2 μM Cd for 24 h, while WT plants exposed to 5 μM Cd did not (Fig. 2A), even though roots of both genotypes contained similar Cd concentrations (Table 1). Moreover, while the Cd translocation factor remained lower in *cad2* mutants than in WT plants after long-term exposure, rosette expansion was still affected more

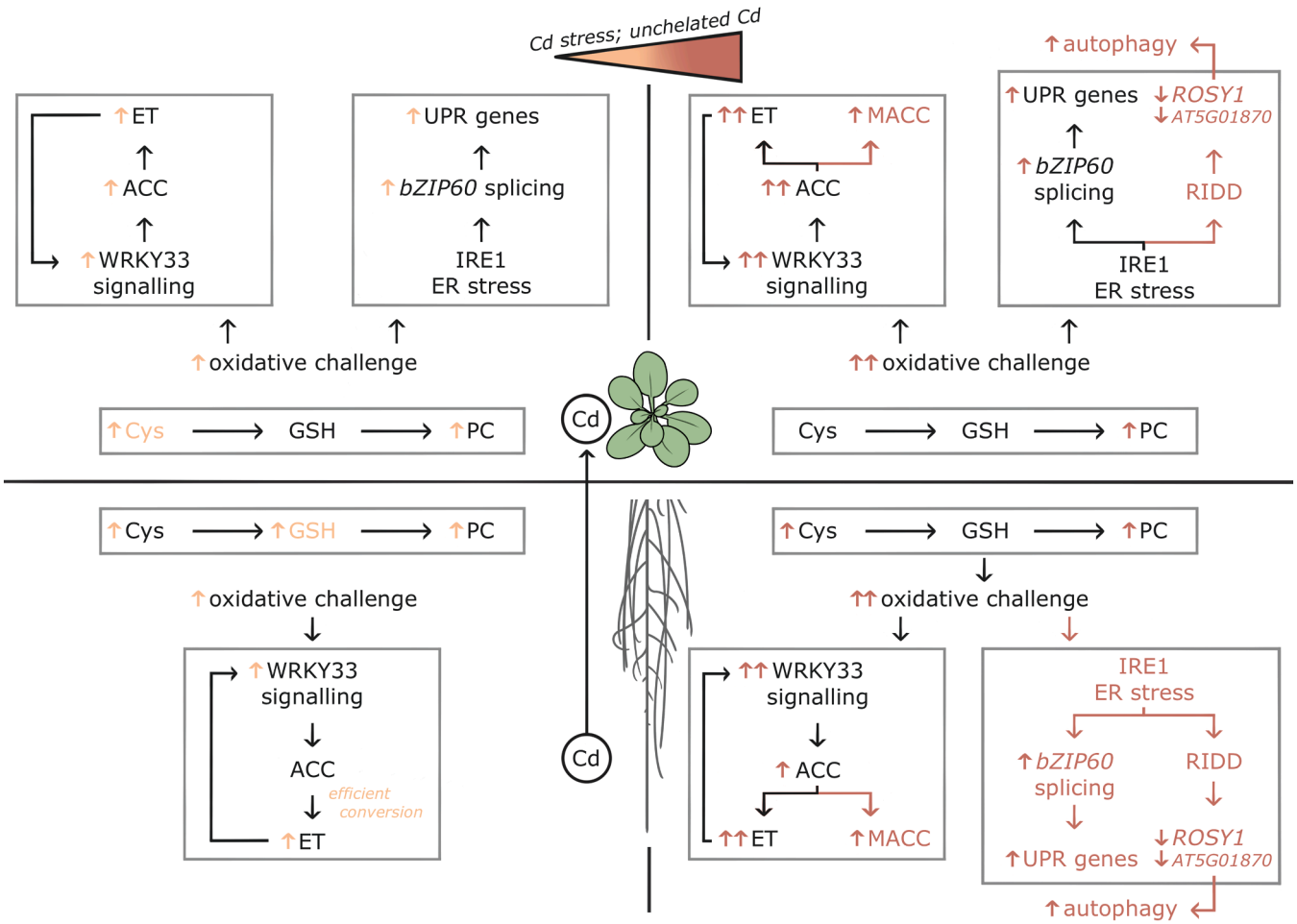

Fig. 8. Proposed model for the acute stress response in leaves (top) and roots (bottom) of *Arabidopsis thaliana* plants exposed to cadmium (Cd) for 24 h at their root level. The condition under mild stress, based on responses of wild-type (WT) plants exposed to 2 μM Cd, is indicated using orange arrows on the left side of the figure. The right side of the figure shows changing responses with increasing Cd stress, based on WT plants exposed to 5 μM Cd and the use of Cd-sensitive *cad* mutants. Responses specific to the mild and more severe Cd stress responses are highlighted in orange and red text, respectively. Overlapping responses are shown in black text, with one red arrow compared to one orange arrow pointing to a similar response between both Cd stress intensities and two red arrows compared to one orange arrow indicating a stronger response upon increasing Cd stress intensity. An upward arrow reflects a stimulation of a process by Cd exposure, while a downward arrow reflects a Cd-induced decrease in a process. ACC: 1-aminocyclopropane-1-carboxylic acid, *AT5G01870: pathogenesis-related (PR) protein belonging to the PR-14 family, bZIP60: basic region/leucine zipper motif 60*, Cys: cysteine, ER: endoplasmic reticulum, ET: ethylene, GSH: glutathione, IRE1: inositol requiring 1, MACC: malonyl-ACC, PC: phytochelatin, RIDD: IRE1-dependent decay of mRNA, *ROSY1: interactor of synaptotagmin 1*, UPR: unfolded protein response of the ER, WRKY33: WRKY DNA-binding protein 33.

severely in the mutant (Hendrix et al., 2020). In this light, the (trend) towards a less pronounced Cd-induced upregulation of some oxidative stress marker genes in *cad* mutant leaves compared to WT leaves could be related to a different compartmentation of the Cd stress response (Table 2). Indeed, the stronger induction of *UPOX*, one of the core genes upregulated following mitochondrial stress signalling (De Clercq et al., 2013), in leaves of the *cad* mutants compared to the WT suggests that the Cd stress response in these mutants is particularly severe in certain cellular compartments (Table 2). Taken together, we propose that the Cd stress intensity of these mutants in the current framework is mostly determined by a higher proportion of non-chelated Cd rather than altered Cd distribution as such (Fig. 8).

Apart from serving to verify the dependency of different responses on Cd stress intensity, the parallel comparison of both mutants also allows a distinction between the importance of GSH acting as a PC precursor or serving different functions during Cd stress, as the mutants are (partially) PC-deficient, while their GSH levels are tremendously different (Fig. 3B-C). It should be noted that high GSH levels in the Cd-exposed *cad1–3* mutant, which were in line with previous results (Howden et al., 1995b; Sobrino-Plata et al., 2014), could alternatively reflect a disrupted cytosolic breakdown of glutathione conjugates (Blum et al., 2010). Although shown for xenobiotic GSH conjugates (Blum et al., 2010), the contribution of PCS1 to the cytosolic degradation of endogenous GSH conjugates remains, to the best of our knowledge, unknown. Furthermore, the accumulation of the GSH precursor cysteine next to GSH in the Cd-exposed *cad1–3* mutant rather supports an increased accumulation of PC precursors due to a disrupted flow to PC production rather than a disrupted GSH catabolism (Fig. 3A). As such, we propose that this study indicates that low or absent PC production, and hence their lower chelation of Cd, rather than altered GSH levels (Fig. 3B-C) determines the high Cd sensitivity of the *cad* mutants (Fig. 1). This is corroborated by the finding that treatment with the GSH biosynthesis inhibitor l-buthionine-sulfoximine (BSO) only barely affected the growth of PCS activity-defective *cad1-3* mutant plants, while it greatly reduced that of WT plants (Howden et al., 1995b). Accordingly, PC production was still elevated in the Cd-exposed *cad2* mutant plants (Fig. 3C), even though it further depleted their already lowered GSH levels in roots [Fig. 3B, (Deckers et al., 2021)], suggesting that stimulating PC production is more crucial than maintaining GSH levels during early Cd stress.

Lastly, it should be pointed out that, despite the Cd-mediated inhibition of rosette diameter in WT and *cad* mutant plants, Cd exposure did not affect new leaf formation in WT plants and reduced this parameter to a lower extent than rosette diameter in the *cad* mutants (Fig. 1C-D). Consistently, this was previously observed during Cd stress (Keunen et al., 2011; Hendrix et al., 2020), and suggests that the formation of new leaves during stress might be favourable. This could be related to a previously developed model that young leaves are more tolerant to stress than mature leaves due to lower basal oxidative stress levels as a result of fewer age-related changes (Kanojia et al., 2020), and would be interesting to investigate further.

4.2. Cadmium induces endoplasmic reticulum stress, which can partly be linked to autophagy, in a stress intensity-dependent manner

After verifying the Cd stress intensity framework of the current study, ER stress was investigated. Cadmium concentration-dependent inductions of ER-UPR genes were observed in WT roots and were potentially preceded by *bZIP60s* induction or induced bZIP60-independently (Table 3; Fig. 8), given that their induction by the ER stressor tunicamycin is not fully abrogated in *bzip60* mutant *A. thaliana* seedlings (Iwata et al., 2008). Cadmium exposure also induced ER stress-related genes in *A. thaliana* seedlings (De Benedictis et al., 2023) and chaperones in *Solanum nigrum* leaves (Song et al., 2023b) in a concentration-dependent manner. Accordingly, the investigated ER-UPR genes, *bZIP60us*, and *bZIP60s* were induced to a higher extent in roots of the *cad* mutants (Table 3). Given the role of GSH in ER homeostasis (Ozgur et al., 2018) and the stimulation of GSH biosynthesis in response to ER stress in *A. thaliana* (Ozgur et al., 2014; Uzilday et al., 2018), the more severe response in Cd-exposed *cad2* mutant roots could be related to their GSH deficiency that is worsened by Cd exposure (Fig. 3B; Table 3). Nevertheless, the similar expression of ER stress-related genes in WT and *cad2* mutant plants under control conditions (Supplemental Table S3), which is in line with similar BiP protein accumulation in *gsh2* mutant *A. thaliana* (Au et al., 2012), suggests that GSH deficiency by itself is insufficient to trigger ER stress. As ER stress genes were also more strongly induced in roots of the Cd-exposed, GSH-accumulating *cad1–3* mutant than in WT roots (Fig. 3B; Table 3), we hence propose that at least part of the strong ER stress responses of *cad* mutant roots are due to their low level of lack of PCs and severe oxidative challenge (Fig. 3C; Table 3).

Remarkably, and in contrast to roots, all investigated ER stress response genes were prominently induced by both mild and moderate Cd stress in leaves of WT plants (Table 3; Fig. 8). Despite it being known that Cd can induce structural changes in the ER (Wierzbicka et al., 2007; Fan et al., 2011), it is, to the best of our knowledge, elusive whether Cd enters this organelle in plants. However, the seemingly higher ER stress responsiveness in leaves compared to roots of WT plants in our study (Table 3), despite similar Cd concentrations in both organs (Table 1), suggests that alternative, indirect mechanisms also contribute to Cd-induced ER stress. For instance, the induction of ER stress genes in WT leaves following mild Cd stress might be related to their more extensive induction of oxidative stress hallmark genes (Table 2), as ROS – including those originating from chloroplasts, mitochondria and peroxisomes – affect the ER stress response (Ozgur et al., 2015). Indeed, SAL1, a regulator of chloroplast retrograde signalling (Estavillo et al., 2011), also contributes to the Cd-mediated induction of ER stress-responsive genes in *A. thaliana* (Xi et al., 2016), highlighting that connections between organellar signalling and the UPR should further be investigated during Cd stress, especially at the leaf level. Nevertheless, it cannot be excluded that mild Cd stress also induced a significant ER stress response in a specific root zone, diluting responses observed at the entire root level (Table 3). This is possible as the earliest tunicamycin-mediated increase in *BiP3* expression was found in specific root zones, and appeared to more rapidly distribute over entire cotyledons than over entire roots of *A. thaliana* seedlings (Cho and Kanehara, 2017). While Cd-exposed leaves were more ER stress-responsive than roots, the extent of their ER-UPR response also appeared to more quickly reach a limit upon increasing Cd stress. As such, the ratio between *bZIP60s* and *bZIP60us* increased to a similar extent in leaves of Cd-exposed WT and *cad* mutant plants, while the inductions of the targets *BiP3* and *ERO1* were less pronounced in mutant leaves (Table 3). Correspondingly, ER stress-related genes were generally upregulated to a lower extent by tunicamycin in *Sorghum bicolor* when a higher concentration of this ER stressor was used (Cavalcante et al., 2023). Correspondingly, a similar expression pattern for ER stress-related genes in *A. thaliana* treated with various concentrations of hydrogen peroxide (Ozgur et al., 2015) further supports that the ER-UPR was overwhelmed in leaves of Cd-exposed *cad* mutant plants compared to WT plants (Table 3).

Next to the aforementioned ER-UPR, transcript levels of *ROSY1* and *AT5G01870* were investigated next, as these transcripts were identified to be among the most vulnerable targets of RIDD in response to tunicamycin (Bao et al., 2018). We found that moderate, but not mild, Cd stress reduced *ROSY1* transcript levels in Cd-exposed WT plants (Table 3; Fig. 8). As this was confirmed to occur IRE1-dependently in leaves (Supplemental Figure S3B), the most ER stress-prone organ (Table 3), we suggest that RIDD (at least of *ROSY1*) becomes particularly significant following more intense Cd stress. Notably, the expression of *bZIP60s* and *bZIP60us* as well as their ratio already increased in WT leaves upon exposure to the lowest Cd concentration and were, in contrast to *AT5G01870* and *ROSY1*, not affected more severely in leaves of Cd-exposed *cad1–3* mutant plants (Table 3; Supplemental Figure S2). As such, our results imply that both IRE1 functions are not necessarily stimulated concomitantly in leaves during Cd stress. In accordance with this suggestion, the *bZIP60* splicing and RIDD functions of IRE1 appear to be able to act independently according to the stressor and stress intensity, as they were activated to different extents and after different durations following exposure to heat, tunicamycin or dithiothreitol in *A. thaliana* (Mishiba et al., 2013). Notably, glycerol treatment, which was found to enhance both RIDD and *bZIP60* splicing in WT *A. thaliana*, could still activate RIDD but not *bZIP60* splicing in an *ire1a/ire1b* mutant complemented with IRE1B lacking an ER luminal sensor domain. This confirms the existence of different activation mechanisms for both IRE1 functions and indicates that RIDD may also act independently of luminal ER stress sensing (Mishiba et al., 2019).

In accordance with the decreased transcript level of *ROSY1*, autophagy was stimulated at the transcript and protein levels by exposure to 5 μM Cd in WT plants (Fig. 4; Fig. 8; Table 4). This was especially evident at the leaf level, thereby again raising the question of whether leaves are more Cd stress responsive compared to roots, as appeared to be the case for the ER-UPR (Table 3), or whether these stress responses are mostly induced in specific root zones of Cd-exposed plants. Regardless, these results are in line with more *ATGs* being upregulated in leaves compared to roots of *Citrus sinensis* after five days of exposure to Cd (Fu et al., 2020). As *ATG8H* was the most Cd-responsive *ATG8* gene [Table 4, (Calero-Muñoz et al., 2019)], Cd-induced autophagy was further verified by concanamycin A-dependent accumulation of GFP-ATG8H puncta in trichoblasts with early root hair formation after 5 μM Cd exposure (Supplemental Figure S4). Although autophagic structures were previously reported in plants following Cd stress (de Araújo et al., 2017; Gzyl et al., 2017; Calero-Muñoz et al., 2019; Meng et al., 2024), we believe this is the first indication that moderate Cd stress stimulates autophagosome production rather than impacting autophagic body degradation in plants (Supplemental Figure S4). This is also in line with the Cd-exposed plants investing in *ATG* upregulation (Table 4), which was also observed in other plant species such as *Brassica rapa* (Meng et al., 2024) and *Malus domestica* (Huo et al., 2022). Furthermore, transcript and protein data in the most severely stressed *cad1-3* mutant support a dependency of autophagy on the Cd stress intensity (Fig. 4; Fig. 8; Table 4), in accordance with the Cd concentration-dependent stimulation of this process that was previously observed in *B. rapa* roots (Meng

et al., 2024). In agreement with the finding that AT5G01870 and ROSY1 can inhibit autophagy (Bao et al., 2018), these autophagy-related parameters were negatively correlated with the expression of *AT5G01870* and *ROSY1* in the framework of the current study (Fig. 5; Fig. 8). As these transcripts were reported to be especially vulnerable RIDD targets (Bao et al., 2018) and as Cd induces ER stress (Table 3), it is not surprising that these correlations were no longer evident when only using data from unexposed plants (Supplemental Table S4). While the correlations cannot ascertain that one parameter preceded the other or that Cd did not affect both parameters independently of one another, the abrogated *ATG8H* induction in leaves of Cd-exposed *ire1a/ire1b* double mutants does confirm that there is a connection between IRE1 and autophagy in Cd-exposed leaves, which may occur via RIDD (Supplemental Figure S3). To our knowledge, peroxisomes are the only reported targets of Cd-induced autophagy in plants so far (Calero-Muñoz et al., 2019). Therefore, a potential connection between Cd-induced autophagy and another organelle, such as the ER, brings forth a relevant topic for future research. As the ER itself can also be targeted by autophagy (Liu et al., 2012; Yoshitake et al., 2022) and *bZIP60* splicing was higher in roots of an *atg10* mutant compared to WT *Z. mays* after treatment with the ER stressor DTT (Tang et al., 2024), it would be interesting to determine whether a connection between ER stress and autophagy during Cd stress is reciprocal.

Lastly, it should be noted that, while the degree of ATG8 lipidation was not significantly different between the Cd-exposed *cad2* mutant and its WT (Fig. 4), *ATG* expression was differentially affected. While their overall upregulation was largely similar between roots of Cd-exposed WT and *cad2* mutant plants, several genes were more or less severely upregulated in the mutant (Table 4). As such, even if the extent of autophagy was not differentially affected, there may still be a shift in the contribution of different *ATG8* genes to the Cd stress response (Table 4), which should be dissected further as the ATG8s were recently demonstrated to have differential specialisations (Del Chiaro et al., 2024). In contrast to roots, *ATG8* induction was generally less pronounced in leaves of Cd-exposed *cad2* mutant compared to WT plants (Table 4). This may be related to the higher basal expression of multiple *ATG8* genes and soluble ATG8 proteins in leaves of this GSH-deficient mutant compared to its WT under control conditions (Fig. 4A; Supplemental Table S3), which may have rendered the mutant less able to cope with its increased stress by stimulating autophagy at the transcriptional level. Likewise, the addition of GSH alleviated ER stress-induced increases in ATG8 gene and protein abundance in *Chlamydomonas reinhardtii* (Pérez-Martín et al., 2014), further supporting that a lowered GSH level may have already compromised the *cad2* mutant under basal conditions.

4.3. *More severe cadmium stress elevates the biosynthesis of ethylene and its precursor 1-aminocyclopropane-1-carboxylic acid, also shunting the latter towards enhanced conjugation*

As the phytohormone ethylene is important during the Cd stress response and can be linked to the oxidative environment, ER, and autophagy (Iven et al., 2023), it was last investigated in the Cd stress intensity framework of this study. In WT plants, Cd exposure only significantly increased free ACC levels in leaves but not in roots (Fig. 7A). This is consistent with earlier observations that *A. thaliana* roots are more sensitive to ACC and ethylene (Vanderstraeten et al., 2019), and that they generally maintain lower ACC levels compared to shoots (Cao et al., 2024). Nevertheless, despite their lack of ACC accumulation, Cd-exposed WT roots may still show enhanced ethylene production. Indeed, the increased expression of *ACO2* and *ERF1*, which are ethylene-responsive (Raz and Ecker, 1999; Lorenzo et al., 2003), in Cd-exposed WT roots does point towards a stimulated ethylene response. Furthermore, *WRKY33* was significantly upregulated in Cd-exposed WT roots (Table 5). Apart from encoding a transcription factor that enhances *ACS2* expression (Li et al., 2012), *WRKY33* was also identified to be part of the shoot ethylene-responsive gene set (Sanchez-Muñoz et al., 2024). As such, the lack of significant increases in ACC levels may simply point towards a more efficient conversion of this metabolite to ethylene. In line with this hypothesis, a model was put forward where higher levels of ACC overflow ACO (Vanderstraeten et al., 2019) and it was suggested that ACO, rather than ACS, acts as the rate-limiting enzyme of ethylene biosynthesis in post-climacteric *Solanum lycopersicum* fruit (Van de Poel et al., 2012). Additionally, this also puts forward the question whether accumulated ACC might then elicit ethylene-independent effects, as ACC-dependent and ethylene-independent responses were identified previously (Vanderstraeten et al., 2019).

Increasing Cd stress intensities induced by using the *cad* mutants showed, with the exception of the Cd-exposed *cad2* mutant leaves, more pronounced upregulations of *ACS2* and *WRKY33* and larger increases in free ACC levels compared to their WT counterparts (Table 5). As WRKY33 is regulated by MPK3 and MPK6 (Mao et al., 2011) that can, in turn, be activated by hydrogen peroxide-responsive oxidative signal inducible 1 (OXI1) kinase (Rentel et al., 2004), this suggests a contribution of the severely affected oxidative environment of the Cd-exposed mutants to ACC biosynthesis (Fig. 8). This is further supported by the higher *OXI1* induction and ACC levels in roots of *cad2* mutants compared to WT plants after exposure to 5 μM Cd for 72 h (Deckers et al., 2021). Additionally, Sanchez-Muñoz et al. (2024) found that WRKY33 is a central regulator of stress signalling in leaves that interacts with the upstream regulator of MPK6 (i.e. MPK kinase 9, MKK9) and is ethylene-responsive, highlighting the interconnection between ethylene biosynthesis and signalling as well as oxidative signalling. Consistent with increased *WRKY33* expression and ACC biosynthesis upon increasing Cd stress, the Cd-exposed *cad* mutants showed a higher ethylene emission compared to WT plants (Fig. 6). As it was not feasible to distinguish between ethylene emission from roots or leaves, no definite conclusions can be made regarding their origin. Nevertheless, larger upregulations of at least one ethylene-responsive gene for leaves and roots of the Cd-exposed *cad* mutants compared to their WT counterparts do point towards a more severe ethylene response with increasing Cd stress severity in both organs that may potentially sustain itself (Fig. 8; Table 5). This is further corroborated by the earlier finding that the expression of ethylene-responsive genes increased with higher Cd concentrations in *A. thaliana* seedlings (Abozeid et al., 2017). At least for *A. thaliana* roots, however, this does seem to reach a limit, as Cd only increased the signal from an ethylene-responsive reporter (EBS::GUS) up until a certain concentration (Bahmani et al., 2022).

Apart from the leaves of Cd-exposed *cad2* mutant plants, larger increases in free ACC levels were accompanied by larger increases in the conjugation of ACC to form MACC (Fig. 7B). Notably, this conjugate also accumulated to larger extents in leaves and roots of *ethylene-overproducer* (*eto1* and *eto3*) mutants compared to WT *A. thaliana* plants (Cao et al., 2024) and may serve to negatively regulate ethylene production (Van de Poel et al., 2014; Cao et al., 2024). To our knowledge, this is the first demonstration that Cd stress increases MACC levels in plants. Nevertheless, our results are in line with earlier observations that higher Cd concentrations elevated conjugated ACC levels (determined by acid hydrolysis of the extract) in *A. thaliana* (Schellingen et al., 2014). Given that ROS-ethylene interactions were proposed to be at the tipping point between cell survival and death during stress responses (Depaepe et al., 2021), this increased ACC conjugation could serve as a protective mechanism to limit an excessive and detrimental ethylene burst during Cd stress. This hypothesis is in line with the observation that leaves of the more severely Cd-stressed *cad2* mutant (Fig. 1) shunted their ACC pool more strongly towards conjugation, potentially reducing the Cd-induced increase in their free ACC levels compared to their WT counterparts (Fig. 7). Indeed, the similar Cd-induced increases in *WRKY33* and *ACS2* expression between leaves of *cad2* mutant and WT plants also support that biosynthesis of ACC was not hampered in this mutant (Table 5) but rather served an alternative fate. Given this hypothesis, it may seem surprising that leaves of the Cd-exposed *cad1–3*

mutant and roots of both Cd-exposed *cad* mutants showed more severe increases in both ACC and MACC levels and larger *ACS2* upregulations than their WT counterparts (Fig. 7). Nevertheless, it is possible that, from a certain Cd stress level, as in these mutants, the burst in ACC biosynthesis is too excessive to be counteracted by ACC conjugation. Correspondingly, while Deckers et al. (2021) also observed a weaker increase in free ACC levels of *cad2* mutant compared to WT leaves after 24 h Cd exposure, ACC levels in this mutant already caught up to those of WT plants after prolonged (72 h) exposure. In line with our suggestion, Michaelis-Menten kinetics were observed in vitro for the *S. lycopersicum* MACC-forming enzyme ACC malonyl-transferase (AMT) with ACC addition (Martin and Saftner, 1995). Although unknown whether and how this translates to physiological conditions, this result supports that there is a limit to AMT activity increasing with ACC availability. As such, while our results highlight a higher shunting of free ACC to MACC with more severe Cd stress, it would be interesting to further uncover how this affects the ethylene response and plant acclimation to the stress condition.

5. Conclusion

Through the combined use of different Cd concentrations and Cd-sensitive *cad2* and *cad1–3* mutants that respectively produce less or no PCs during Cd stress, we highlighted the differentiating responses related to ER stress, autophagy, ethylene and its precursor ACC during acute Cd stress in *A. thaliana*. Upon increasing Cd concentrations in WT plants, PC production appeared to reach a limit, thereby potentially leaving more Cd unchelated and readily available to elicit damage (Fig. 8). In addition, we propose that the interference with Cd chelation by PCs is the main contributor to the more severe responses observed in the Cd-sensitive *cad* mutants plants used throughout our study, corroborating the significance of the function of GSH as a PC precursor in the early defence against Cd exposure. Accordingly, our experimental set-up of varying Cd concentrations and *cad* mutants allowed us to observe a dependence of the IRE1-regulated ER-UPR, related to *bZIP60* splicing (*bZIP60s*), on Cd stress intensity in roots. While the *bZIP60s* branch was more responsive to Cd at lower concentrations in WT leaves than in roots (at least when studying the entire root level), the induction of the ER-UPR also appeared to reach a limit in leaves upon increasing Cd stress that was unobserved for roots (Fig. 8). On the other hand, decreases in the transcript levels of the autophagy-inhibiting RIDD targets *ROSY1* and *AT5G01870* appeared relevant from moderate Cd stress (i.e. 5 μM Cd in WT plants) onwards and were, in contrast to the ER-UPR, still aggravated in leaves of the *cad* mutant plants experiencing more severe Cd stress (Fig. 8). As we confirmed that *ROSY1* downregulation in leaves of Cd-exposed plants can indeed be attributed to IRE1, our results suggest that both IRE1 functions are regulated differently in leaves depending on the Cd stress intensity. Furthermore, the Cd-induced decreases in these autophagy-inhibiting transcripts correlated with the upregulation of autophagy-related genes and the degree of ATG8 lipidation during Cd stress (Fig. 8). Therefore, we propose that ER stress may be an important determinant of Cd-induced autophagy and should be investigated in more detail. Furthermore, we found that free ACC levels generally accumulate upon increasing Cd stress, potentially due to increased ACC biosynthesis as a result of an increased oxidative challenge and less efficient conversion to ethylene (Fig. 8). While higher ethylene emission could still occur upon increasing Cd stress, it may also have been limited by an increased conjugation of free ACC, forming MACC, highlighting the need to further uncover the interplay between this ACC conjugate and the strength of the ethylene response during Cd stress (Fig. 8).

CRediT authorship contribution statement

Isabeau Vanbuel: Writing – original draft, Visualization, Investigation, Funding acquisition, Formal analysis, Conceptualization. **Verena Iven:** Writing – review & editing, Investigation, Formal analysis, Conceptualization. **Thomas Depaepe:** Writing – review & editing, Investigation, Formal analysis. **Martijn Heleven:** Writing – review & editing, Investigation. **Marijke Jozefczak:** Writing – review & editing, Investigation, Formal analysis. **Karen Smeets:** Writing – review & editing, Methodology. **Luis E. Hernández:** Formal analysis, Investigation, Methodology, Supervision, Writing – review & editing. **Els Prinsen:** Writing – review & editing, Methodology, Investigation, Funding acquisition, Formal analysis. **Dominique Van Der Straeten:** Writing – review & editing, Methodology, Funding acquisition. **Sophie Hendrix:** Writing – review & editing, Supervision, Investigation, Formal analysis, Conceptualization. **Ann Cuypers:** Writing – review & editing, Supervision, Project administration, Funding acquisition, Conceptualization.

Declaration of competing interest

The authors declare that they have no known competing financial interests or personal relationships that could have appeared to influence the work reported in this paper.

Funding

This work was funded by the Special Research Fund (BOF) of Hasselt University through a PhD grant to Isabeau Vanbuel (grant number BOF20DOC08). Additional funding came from an Interuniversity BOF project to DVDS, AC and EP (grant number IBOF/23/070).

Acknowledgements

We are grateful to Prof. Dr Michelle Plusquin and Dr Brigitte Reimann for their input on correlation analyses, as well as Birk Auwerkerken and Dario Geebelen for their work during their internships. Laura Bos Calderó, Jasmine Colemont, Kris Kunnen, Sevgi Öden, Carine Put, Seb Tombeur, Dominika Tylus, Ann Wijgaerts and Tim Willems are thanked for their assistance.

Supplementary materials

Supplementary material associated with this article can be found, in the online version, at doi:10.1016/j.stress.2025.100996.

Data availability

Data will be made available on request.

References

Abozeid, A., Ying, Z., Lin, Y., Liu, J., Zhang, Z., Tang, Z., 2017. Ethylene improves root system development under cadmium stress by modulating superoxide anion concentration in Arabidopsis thaliana. Front. Plant Sci. 8, 253. https://doi.org/10.3389/fpls.2017.00253.

Au, K.K.C., Pérez-Gómez, J., Neto, H., Müller, C., Meyer, A.J., Fricker, M.D., Moore, I., 2012. A perturbation in glutathione biosynthesis disrupts endoplasmic reticulum morphology and secretory membrane traffic in Arabidopsis thaliana. The Plant Journal 71 (6), 881–894. https://doi.org/10.1111/j.1365-313X.2012.05022.x.

Bahmani, R., Kim, D., Modareszadeh, M., Hwang, S., 2022. Cadmium enhances root hair elongation through reactive oxygen species in Arabidopsis. Environ. Exp. Bot. 196, 104813. https://doi.org/10.1016/j.envexpbot.2022.104813.

Ballabio, C., Jones, A., Panagos, P., 2024. Cadmium in topsoils of the European Union - An analysis based on LUCAS topsoil database. Science of the Total Environment 912, 168710. https://doi.org/10.1016/j.scitotenv.2023.168710.

Bao, Y., Pu, Y., Yu, X., Gregory, B.D., Srivastava, R., Howell, S.H., Bassham, D.C., 2018. IRE1B degrades RNAs encoding proteins that interfere with the induction of autophagy by ER stress in Arabidopsis thaliana. Autophagy. 14 (9), 1562–1573. https://doi.org/10.1080/15548627.2018.1462426.

Blum, R., Meyer, K.C., Wünschmann, J., Lendzian, K.J., Grill, E., 2010. Cytosolic action of phytochelatin synthase. Plant Physiol. 153 (1), 159–169. https://doi.org/10.1104/pp.109.149922.

Bustin, S.A., Benes, V., Garson, J.A., Hellemans, J., Huggett, J., Kubista, M., Mueller, R., Nolan, T., Pfaffl, M.W., Shipley, G.L., Vandesompele, J., Wittwer, C.T., 2009. The MIQE guidelines: Minimum Information for publication of Quantitative real-time

PCR Experiments. Clin. Chem. 55 (4), 611–622. https://doi.org/10.1373/clinchem.2008.112797.
Calero-Muñoz, N., Exposito-Rodriguez, M., Collado-Arenal, A.M., Rodríguez-Serrano, M., Laureano-Marín, A.M., Santamaría, M.E., Gotor, C., Díaz, I., Mullineaux, P.M., Romero-Puertas, M.C., Olmedilla, A., Sandalio, L.M., 2019. Cadmium induces reactive oxygen species-dependent pexophagy in Arabidopsis leaves. Plant Cell Environ. 42 (9), 2696–2714. https://doi.org/10.1111/pce.13597.
Cao, D., Depaepe, T., Sanchez-Muñoz, R., Janssens, H., Lemière, F., Willems, T., Winne, J., Prinsen, E., Van Der Straeten, D., 2024. A UPLC-MS/MS method for quantification of metabolites in the ethylene biosynthesis pathway and its biological validation in Arabidopsis. New Phytologist 243 (3), 1262–1275. https://doi.org/10.1111/nph.19878.
Cao, J., Wang, C., Hao, N., Fujiwara, T., Wu, T., 2022. Endoplasmic reticulum stress and reactive oxygen species in plants. Antioxidants. (Basel) 11 (7), 1240. https://doi.org/10.3390/antiox11071240.
Cavalcante, F.L.P., da Silva, S.J., de Sousa Lopes, L., de Oliveira Paula-Marinho, S., Guedes, M.I.F., Gomes-Filho, E., de Carvalho, H.H., 2023. Unveiling a differential metabolite modulation of Sorghum varieties under increasing tunicamycin-induced endoplasmic reticulum stress. Cell Stress and Chaperones 28 (6), 889–907. https://doi.org/10.1007/s12192-023-01382-5.
Chen, J., Wang, X., Zhang, W., Zhang, S., Zhao, F.J., 2020. Protein phosphatase 2A alleviates cadmium toxicity by modulating ethylene production in Arabidopsis thaliana. Plant Cell Environ. 43 (4), 1008–1022. https://doi.org/10.1111/pce.13716.
Cho, Y., Kanehara, K., 2017. Endoplasmic reticulum stress response in Arabidopsis roots. Front. Plant Sci. 8. https://doi.org/10.3389/fpls.2017.00144.
Cobbett, C.S., May, M.J., Howden, R., Rolls, B., 1998. The glutathione-deficient, cadmium-sensitive mutant, cad2-1, of Arabidopsis thaliana is deficient in γ-glutamylcysteine synthetase. The Plant Journal 16 (1), 73–78. https://doi.org/10.1046/j.1365-313x.1998.00262.x.
Cuypers, A., Vanbuel, I., Iven, V., Kunnen, K., Vandionant, S., Huybrechts, M., Hendrix, S., 2023. Cadmium-induced oxidative stress responses and acclimation in plants require fine-tuning of redox biology at subcellular level. Free Radical Biology and Medicine 199, 81–96. https://doi.org/10.1016/j.freeradbiomed.2023.02.010.
Czékus, Z., Szalai, G., Tari, I., Khan, M.I.R., Poór, P., 2022. Role of ethylene in ER stress and the unfolded protein response in tomato (Solanum lycopersicum L.) plants. Plant Physiology and Biochemistry 181, 1–11. https://doi.org/10.1016/j.plaphy.2022.03.031.
de Araújo, R.P., de Almeida, A.A.F., Pereira, L.S., Mangabeira, P.A.O., Souza, J.O., Pirovani, C.P., Ahnert, D., Baligar, V.C., 2017. Photosynthetic, antioxidative, molecular and ultrastructural responses of young cacao plants to Cd toxicity in the soil. Ecotoxicol. Environ. Saf. 144, 148–157. https://doi.org/10.1016/j.ecoenv.2017.06.006.
De Benedictis, M., Gallo, A., Migoni, D., Papadia, P., Roversi, P., Santino, A., 2023. Cadmium treatment induces endoplasmic reticulum stress and unfolded protein response in Arabidopsis thaliana. Plant Physiology and Biochemistry 196, 281–290. https://doi.org/10.1016/j.plaphy.2023.01.056.
De Clercq, I., Vermeirssen, V., Van Aken, O., Vandepoele, K., Murcha, M.W., Law, S.R., Inzé, A., NgS., Ivanova, A., Rombaut, D., van de Cotte, B., Jaspers, P., Van de Peer, Y., Kangasjärvi, J., Whelan, J., Van Breusegem, F., 2013. The membrane-bound NAC transcription factor ANAC013 functions in mitochondrial retrograde regulation of the oxidative stress response in Arabidopsis. Plant Cell 25 (9), 3472–3490. https://doi.org/10.1105/tpc.113.117168.
Deckers, J., Hendrix, S., Prinsen, E., Vangronsveld, J., Cuypers, A., 2020. Identifying the pressure points of acute cadmium stress prior to acclimation in Arabidopsis thaliana. Int. J. Mol. Sci. 21 (17), 6232. https://doi.org/10.3390/ijms21176232.
Deckers, J., Hendrix, S., Prinsen, E., Vangronsveld, J., Cuypers, A., 2021. Glutathione is required for the early alert response and subsequent acclimation in cadmium-exposed Arabidopsis thaliana plants. Antioxidants 11 (1), 6. https://doi.org/10.3390/antiox11010006.
Del Chiaro, A., Grujic, N., Zhao, J., Papareddy, R.K., Gao, P., Ma, J., Löfke, C., Bhattacharya, A., Gruetzner, R., Bourguet, P., Berger, F., Kang, B.H., Marillonnet, S., Dagdas, Y., 2024. Nonuple atg8 mutant provides genetic evidence for functional specialisation of ATG8 isoforms in Arabidopsis thaliana. bioRxiv (preprint). https://doi.org/10.1101/2024.12.10.627464.
Demircan, N., Ozgur, R., Turkan, I., Uzilday, B., 2024. Heavy metal toxicity leads to accumulation of insoluble proteins and induces endoplasmic reticulum stress–specific unfolded protein response in Arabidopsis thaliana. Environmental Science and Pollution Research 31 (40), 53206–53218. https://doi.org/10.1007/s11356-024-34780-y.
Deng, Y., Humbert, S., Liu, J.X., Srivastava, R., Rothstein, S.J., Howell, S.H., 2011. Heat induces the splicing by IRE1 of a mRNA encoding a transcription factor involved in the unfolded protein response in Arabidopsis. Proc. Natl. Acad. Sci. u S. a 108 (17), 7247–7252. https://doi.org/10.1073/pnas.1102117108.
Depaepe, T., Hendrix, S., Janse van Rensburg, H.C., Van den Ende, W., Cuypers, A., Van Der Straeten, D., 2021. At the crossroads of survival and death: The reactive oxygen species-ethylene-sugar triad and the unfolded protein response. Trends. Plant Sci. 26 (4), 338–351. https://doi.org/10.1016/j.tplants.2020.12.007.
Ducruix, C., Junot, C., Fiévet, J.B., Villiers, F., Ezan, E., Bourguignon, J., 2006. New insights into the regulation of phytochelatin biosynthesis in A. thaliana cells from metabolite profiling analyses. Biochimie 88 (11), 1733–1742. https://doi.org/10.1016/j.biochi.2006.08.005.
Estavillo, G.M., Crisp, P.A., Pornsiriwong, W., Wirtz, M., Collinge, D., Carrie, C., Giraud, E., Whelan, J., David, P., Javot, H., Brearley, C., Hell, R., Marin, E., Pogson, B.J, 2011. Evidence for a SAL1-PAP Chloroplast Retrograde Pathway That Functions in Drought and High Light Signaling in Arabidopsis. Plant Cell 23 (11), 3992–4012. https://doi.org/10.1105/tpc.111.091033.
Fan, J.L., Wei, X.Z., Wan, L.C., Zhang, L.Y., Zhao, X.Q., Liu, W.Z., Hao, H.Q., Zhang, H.Y., 2011. Disarrangement of actin filaments and Ca^{2+} gradient by $CdCl_2$ alters cell wall construction in Arabidopsis thaliana root hairs by inhibiting vesicular trafficking. J. Plant Physiol. 168 (11), 1157–1167. https://doi.org/10.1016/j.jplph.2011.01.031.
Fu, X.Z., Zhou, X., Xu, Y.Y., Hui, Q.L., Chun, C.P., Ling, L.L., Peng, L.Z., 2020. Comprehensive analysis of autophagy-related genes in sweet orange (Citrus sinensis) highlights their roles in response to abiotic stresses. Int. J. Mol. Sci. 21 (8), 2699. https://doi.org/10.3390/ijms21082699.
Gadjev, I., Vanderauwera, S., Gechev, T.S., Laloi, C., Minkov, I.N., Shulaev, V., Apel, K., Inzé, D., Mittler, R., Van Breusegem, F., 2006. Transcriptomic footprints disclose specificity of reactive oxygen species signalling in Arabidopsis. Plant Physiol. 141 (2), 436–445. https://doi.org/10.1104/pp.106.078717.
Gielen, H., Vangronsveld, J., Cuypers, A., 2017. Cd-induced Cu deficiency responses in Arabidopsis thaliana: Are phytochelatins involved? Plant Cell Environ. 40 (3), 390–400. https://doi.org/10.1111/pce.12876.
Gong, J.M., Lee, D.A., Schroeder, J.I., 2003. Long-distance root-to-shoot transport of phytochelatins and cadmium in Arabidopsis. Proc. Natl. Acad. Sci. u S. a 100 (17), 10118–10123. https://doi.org/10.1073/pnas.1734072100.
Gzyl, J., Chmielowska-Bak, J., Przymusiński, R., 2017. Gamma-tubulin distribution and ultrastructural changes in root cells of soybean (Glycine max L.) seedlings under cadmium stress. Environ. Exp. Bot. 143, 82–90. https://doi.org/10.1016/j.envexpbot.2017.08.011.
Ha, S.B., Smith, A.P., Howden, R., Dietrich, W.M., Bugg, S., O'Connell, M.J., Goldsbrough, P.B., Cobbett, C.S., 1999. Phytochelatin synthase genes from Arabidopsis and the yeast Schizosaccharomyces pombe. Plant Cell 11 (6), 1153–1163. https://doi.org/10.1105/tpc.11.6.1153.
Hendrix, S., Jozefczak, M., Wójcik, M., Deckers, J., Vangronsveld, J., Cuypers, A., 2020. Glutathione: a key player in metal chelation, nutrient homeostasis, cell cycle regulation and the DNA damage response in cadmium-exposed Arabidopsis thaliana. Plant Physiology and Biochemistry 154, 498–507. https://doi.org/10.1016/j.plaphy.2020.06.006.
Howden, R., Andersen, C.R., Goldsbrough, P.B., Cobbett, C.S., 1995a. A cadmium-sensitive, glutathione-deficient mutant of Arabidopsis thaliana. Plant Physiol. 107 (4), 1067–1073. https://doi.org/10.1104/pp.107.4.1067.
Howden, R., Goldsbrough, P.B., Andersen, C.R., Cobbett, C.S., 1995b. Cadmium-sensitive, cad1 mutants of Arabidopsis thaliana are phytochelatin deficient. Plant Physiol. 107 (4), 1059–1066. https://doi.org/10.1104/pp.107.4.1059.
Huo, L.Q., Guo, Z.J., Wang, Q., Jia, X., Sun, X.P., Ma, F.W., 2022. The protective role of MdATG10-mediated autophagy in apple plant under cadmium stress. Ecotoxicol. Environ. Saf. 234, 13. https://doi.org/10.1016/j.ecoenv.2022.113398.
Iven, V., Vanbuel, I., Hendrix, S., Cuypers, A., 2023. The glutathione-dependent alarm triggers signalling responses involved in plant acclimation to cadmium. J. Exp. Bot. 74 (11), 3300–3312. https://doi.org/10.1093/jxb/erad081.
Iwata, Y., Fedoroff, N.V., Koizumi, N., 2008. Arabidopsis bZIP60 is a proteolysis-activated transcription factor involved in the endoplasmic reticulum stress response. Plant Cell 20 (11), 3107–3121. https://doi.org/10.1105/tpc.108.061002.
Jozefczak, M., Keunen, E., Schat, H., Bliek, M., Hernández, L.E., Carleer, R., Remans, T., Bohler, S., Vangronsveld, J., Cuypers, A., 2014. Differential response of Arabidopsis leaves and roots to cadmium: Glutathione-related chelating capacity vs antioxidant capacity. Plant Physiology and Biochemistry 83, 1–9. https://doi.org/10.1016/j.plaphy.2014.07.001.
Kacprzak, S.M., Van Aken, O., 2023. FRIENDLY is required for efficient dark-induced mitophagy and controlled senescence in Arabidopsis. Free Radical Biology and Medicine 204, 1–7. https://doi.org/10.1016/j.freeradbiomed.2023.04.007.
Kanojia, A., Gupta, S., Benina, M., Fernie, A.R., Mueller-Roeber, B., Gechev, T., Dijkwel, P.P., 2020. Developmentally controlled changes during Arabidopsis leaf development indicate causes for loss of stress tolerance with age. J. Exp. Bot. 71 (20), 6340–6354. https://doi.org/10.1093/jxb/eraa347.
Keunen, E., Truyens, S., Bruckers, L., Remans, T., Vangronsveld, J., Cuypers, A., 2011. Survival of Cd-exposed Arabidopsis thaliana: Are these plants reproductively challenged? Plant Physiology and Biochemistry 49 (10), 1084–1091. https://doi.org/10.1016/j.plaphy.2011.07.013.
Li, G., Meng, X., Wang, R., Mao, G., Han, L., Liu, Y., Zhang, S., 2012. Dual-level regulation of ACC synthase activity by MPK3/MPK6 cascade and its downstream WRKY transcription factor during ethylene induction in Arabidopsis. PLoS. Genet. 8 (6), e1002767. https://doi.org/10.1371/journal.pgen.1002767.
Li, J., Wang, L.Y., Huang, H.C., Yang, W., Dai, G.Y., Fang, Z.Q., Zhao, J.L., Xia, K.F., Zeng, X., He, M.L., Yao, N., Zhang, M.Y., 2024. Endoplasmic reticulum stress response modulator OsbZIP39 regulates cadmium accumulation via activating the expression of defensin-like gene OsCAL2 in rice. J. Hazard. Mater. 476, 135007. https://doi.org/10.1016/j.jhazmat.2024.135007.
Li, M., Hao, P., Cao, F., 2017. Glutathione-induced alleviation of cadmium toxicity in Zea mays. Plant Physiology and Biochemistry 119, 240–249. https://doi.org/10.1016/j.plaphy.2017.09.005.
Li, Y.B., Xu, X.M., Qi, G., Cui, D.Z., Huang, C., Sui, X.X., Li, G.Y., Fan, Q.Q., 2023. Mechanisms of autophagy function and regulation in plant growth, development, and response to abiotic stress. The Crop Journal 11 (6), 1611–1625. https://doi.org/10.1016/j.cj.2023.09.005.
Liao, C.Y., Wang, P., Yin, Y., Bassham, D.C., 2022. Interactions between autophagy and phytohormone signaling pathways in plants. FEBS Lett. 596 (17), 2198–2214. https://doi.org/10.1002/1873-3468.14355.
Liu, Y., Burgos, J.S., Deng, Y., Srivastava, R., Howell, S.H., Bassham, D.C., 2012. Degradation of the endoplasmic reticulum by autophagy during endoplasmic

reticulum stress in Arabidopsis. Plant Cell 24 (11), 4635–4651. https://doi.org/10.1105/tpc.112.101535.
Lorenzo, O., Piqueras, R., Sánchez-Serrano, J.J., Solano, R., 2003. Ethylene response factor1 integrates signals from ethylene and jasmonate pathways in plant defense. Plant Cell 15 (1), 165–178. https://doi.org/10.1105/tpc.007468.
Mao, G., Meng, X., Liu, Y., Zheng, Z., Chen, Z., Zhang, S., 2011. Phosphorylation of a WRKY transcription factor by two pathogen-responsive MAPKs drives phytoalexin biosynthesis in Arabidopsis. Plant Cell 23, 1639–1653. https://doi.org/10.1105/tpc.111.084996.
Marshall, R.S., Vierstra, R.D., 2018. Autophagy: The master of bulk and selective recycling. Annu Rev. Plant Biol. 69, 173–208. https://doi.org/10.1146/annurev-arplant-042817-040606.
Martin, M.N., Saftner, R.A., 1995. Purification and characterisation of 1-aminocyclopropane-1-carboxylic acid N-malonyltransferase from tomato fruit. Plant Physiol. 108 (3), 1241–1249. https://doi.org/10.1104/pp.108.3.1241.
Meng, L.I., Shucheng, S.I., Ming, Z., Caijun, W.U., Xufeng, X., 2024. Cd-induced autophagy responses in pakchoi as revealed by transcriptome analysis. Plant Mol. Biol. Report. 42 (1), 165–182. https://doi.org/10.1007/s11105-023-01403-8.
Mishiba, K., Nagashima, Y., Suzuki, E., Hayashi, N., Ogata, Y., Shimada, Y., Koizumi, N., 2013. Defects in IRE1 enhance cell death and fail to degrade mRNAs encoding secretory pathway proteins in the Arabidopsis unfolded protein response. Proc. Natl. Acad. Sci. u S. a 110 (14), 5713–5718. https://doi.org/10.1073/pnas.1219047110.
Mishiba, K.I., Iwata, Y., Mochizuki, T., Matsumura, A., Nishioka, N., Hirata, R., Koizumi, N., 2019. Unfolded protein-independent IRE1 activation contributes to multifaceted developmental processes in Arabidopsis. Life Sci. Alliance 2 (5). https://doi.org/10.26508/lsa.201900459.
Ozgur, R., Turkan, I., Uzilday, B., Sekmen, A.H, 2014. Endoplasmic reticulum stress triggers ROS signalling, changes the redox state, and regulates the antioxidant defence of Arabidopsis thaliana. J. Exp. Bot. 65 (5), 1377–1390. https://doi.org/10.1093/jxb/eru034.
Ozgur, R., Uzilday, B., Iwata, Y., Koizumi, N., Turkan, I., 2018. Interplay between the unfolded protein response and reactive oxygen species: a dynamic duo. J. Exp. Bot. 69 (14), 3333–3345. https://doi.org/10.1093/jxb/ery040.
Ozgur, R., Uzilday, B., Sekmen, A.H., Turkan, I., 2015. The effects of induced production of reactive oxygen species in organelles on endoplasmic reticulum stress and on the unfolded protein response in Arabidopsis. Ann. Bot. 116 (4), 541–553. https://doi.org/10.1093/aob/mcv072.
Pattyn, J., Vaughan-Hirsch, J., Van de Poel, B., 2021. The regulation of ethylene biosynthesis: a complex multilevel control circuitry. New Phytologist 229 (2), 770–782. https://doi.org/10.1111/nph.16873.
Pérez-Martín, M., Pérez-Pérez, M.E., Lemaire, S.D., Crespo, J.L., 2014. Oxidative stress contributes to autophagy induction in response to endoplasmic reticulum stress in Chlamydomonas reinhardtii. Plant Physiol. 166 (2), 997–1008. https://doi.org/10.1104/pp.114.243659.
Raz, V., Ecker, J.R., 1999. Regulation of differential growth in the apical hook of Arabidopsis. Development 126 (16), 3661–3668. https://doi.org/10.1242/dev.126.16.3661.
Remans, T., Keunen, E., Bex, G.J., Smeets, K., Vangronsveld, J., Cuypers, A., 2014. Reliable gene expression analysis by reverse transcription-quantitative PCR: Reporting and minimising the uncertainty in data accuracy. Plant Cell 26 (10), 3829–3837. https://doi.org/10.1105/tpc.114.130641.
Rentel, M.C., Lecourieux, D., Ouaked, F., Usher, S.L., Petersen, L., Okamoto, H., Knight, H., Peck, S.C., Grierson, C.S., Hirt, H., Knight, M.R., 2004. OXI1 kinase is necessary for oxidative burst-mediated signalling in Arabidopsis. Nature 427 (6977), 858–861. https://doi.org/10.1038/nature02353.
Rozen, S., Skaletsky, H., 2000. Primer3 on the WWW for general users and for biologist programmers. In: Misener, S., Krawetz, S.A. (Eds.), Bioinformatics Methods and Protocols: Methods in Molecular Biology™. Humana Press, Totowa, New Jersey, pp. 365–386. https://doi.org/10.1385/1-59259-192-2:365.
Sanchez-Muñoz, R., Depaepe, T., Samalova, M., Hejatko, J., Zaplana, I., Van Der Straeten, D., 2024. The molecular core of transcriptome responses to abiotic stress in plants: a machine learning-driven meta-analysis. bioRxiv (preprint). https://doi.org/10.1101/2024.01.24.576978.
Schellingen, K., Van Der Straeten, D., Remans, T., Vangronsveld, J., Keunen, E., Cuypers, A., 2015. Ethylene signalling is mediating the early cadmium-induced oxidative challenge in Arabidopsis thaliana. Plant Science 239, 137–146. https://doi.org/10.1016/j.plantsci.2015.07.015.
Schellingen, K., Van Der Straeten, D., Vandenbussche, F., Prinsen, E., Remans, T., Vangronsveld, J., Cuypers, A., 2014. Cadmium-induced ethylene production and responses in Arabidopsis thaliana rely on ACS2 and ACS6 gene expression. BMC. Plant Biol. 14, 214. https://doi.org/10.1186/s12870-014-0214-6.
Schneider, C.A., Rasband, W.S., Eliceiri, K.W., 2012. NIH Image to ImageJ: 25 years of image analysis. Nat. Methods 9 (7), 671–675. https://doi.org/10.1038/nmeth.2089.
Seregin, I.V., Kozhevnikova, A.D., 2023. Phytochelatins: Sulfur-containing metal(loid)-chelating ligands in plants. Int. J. Mol. Sci. 24 (3), 2430. https://doi.org/10.3390/ijms24032430.
Sieńko, K., Poormassalehgoo, A., Yamada, K., Goto-Yamada, S., 2020. Microautophagy in plants: Consideration of Its molecular mechanism. Cells 9 (4), 887. https://doi.org/10.3390/cells9040887.
Smeets, K., Ruytinx, J., Van Belleghem, F., Semane, B., Lin, D., Vangronsveld, J., Cuypers, A., 2008. Critical evaluation and statistical validation of a hydroponic culture system for Arabidopsis thaliana. Plant Physiology and Biochemistry 46 (2), 212–218. https://doi.org/10.1016/j.plaphy.2007.09.014.
Sobrino-Plata, J., Carrasco-Gil, S., Abadía, J., Escobar, C., Álvarez-Fernández, A., Hernández, L.E., 2014. The role of glutathione in mercury tolerance resembles its function under cadmium stress in Arabidopsis. Metallomics. 6 (2), 356–366. https://doi.org/10.1039/c3mt00329a.
Song, G., Zhang, J., Wang, Y., Ji, Y., Fang, Z., Cai, Q., Xu, B., 2023a. Overexpression of PvBiP2 improved biomass yield and cadmium tolerance in switchgrass (Panicum virgatum L.). J. Hazard. Mater. 446, 130648. https://doi.org/10.1016/j.jhazmat.2022.130648.
Song, L.Y., Liu, X., Zhang, L.D., Hu, W.J., Xu, C.Q., Li, J., Song, S.W., Guo, Z.J., Sun, C.Y., Tang, H.C., Wang, J.C., Zhu, X.Y., Zheng, H.L., 2023b. Proteomic analysis reveals differential responsive mechanisms in Solanum nigrum exposed to low and high dose of cadmium. J. Hazard. Mater. 448, 130880. https://doi.org/10.1016/j.jhazmat.2023.130880.
Sterckeman, T., Thomine, S., 2020. Mechanisms of cadmium accumulation in plants. CRC. Crit. Rev. Plant Sci. 39 (4), 322–359. https://doi.org/10.1080/07352689.2020.1792179.
Tang, J., Li, Z., Bassham, D.C., 2024. Interplay between autophagy, the unfolded protein response and the cytoplasmic heat stress response during heat stress in maize. bioRxiv (preprint). https://doi.org/10.1101/2024.11.06.622333.
Uzilday, B., Ozgur, R., Sekmen, A.H., Turkan, I., 2018. Endoplasmic reticulum stress regulates glutathione metabolism and activities of glutathione-related enzymes in Arabidopsis. Functional Plant Biology 45 (2), 284–296. https://doi.org/10.1071/fp17151.
Van de Poel, B., Bulens, I., Hertog, M.L.A.T.M., Nicolai, B.M., Geeraerd, A.H., 2014. A transcriptomics-based kinetic model for ethylene biosynthesis in tomato (Solanum lycopersicum) fruit: Development, validation and exploration of novel regulatory mechanisms. New Phytologist 202 (3), 952–963. https://doi.org/10.1111/nph.12685.
Van de Poel, B., Bulens, I., Markoula, A., Hertog, M.L.A.T.M., Dreesen, R., Wirtz, M., Vandoninck, S., Oppermann, Y., Keulemans, J., Hell, R., Waelkens, E., De Proft, M.P., Sauter, M., Nicolai, B.M., Geeraerd, A.H., 2012. Targeted systems biology profiling of tomato fruit reveals coordination of the Yang cycle and a distinct regulation of ethylene biosynthesis during postclimacteric ripening. Plant Physiol. 160 (3), 1498–1514. https://doi.org/10.1104/pp.112.206086.
Vanderstraeten, L., Depaepe, T., Bertrand, S., Van Der Straeten, D., 2019. The ethylene precursor ACC affects early vegetative development independently of ethylene signalling. Front. Plant Sci. 10, 1591. https://doi.org/10.3389/fpls.2019.01591.
Vanderstraeten, L., Van Der Straeten, D., 2017. Accumulation and transport of 1-aminocyclopropane-1-carboxylic acid (ACC) in plants: Current status, considerations for future research and agronomic applications. Front. Plant Sci. 8, 38. https://doi.org/10.3389/fpls.2017.00038.
Wang, K.L.C., Li, H., Ecker, J.R., 2002. Ethylene biosynthesis and signalling networks. Plant Cell 14, S131–S151. https://doi.org/10.1105/tpc.001768.
Wierzbicka, M.H., Przedpelska, E., Ruzik, R., Ouerdane, L., Poleć-Pawlak, K., Jarosz, M., Szpunar, J., Szakiel, A., 2007. Comparison of the toxicity and distribution of cadmium and lead in plant cells. Protoplasma 231, 99–111. https://doi.org/10.1007/s00709-006-0227-6.
Xi, H., Xu, H., Xu, W., He, Z., Xu, W., Ma, M., 2016. A SAL1 loss-of-function Arabidopsis mutant exhibits enhanced cadmium tolerance in association with alleviation of endoplasmic reticulum stress. Plant and Cell Physiology 57 (6), 1210–1219. https://doi.org/10.1093/pcp/pcw069.
Yoshimoto, K., Hanaoka, H., Sato, S., Kato, T., Tabata, S., Noda, T., Ohsumi, Y., 2004. Processing of ATG8s, ubiquitin-like proteins, and their deconjugation by ATG4s are essential for plant autophagy. Plant Cell 16 (11), 2967–2983. https://doi.org/10.1105/tpc.104.025395.
Yoshitake, Y., Shinozaki, D., Yoshimoto, K., 2022. Autophagy triggered by iron-mediated ER stress is an important stress response to the early phase of Pi starvation in plants. The Plant Journal 110 (5), 1370–1381. https://doi.org/10.1111/tpj.15743.
Yue, J.Y., Wei, X.J., Wang, H.Z., 2018. Cadmium tolerant and sensitive wheat lines: their differences in pollutant accumulation, cell damage, and autophagy. Biologia Plantarum 62 (2), 379–387. https://doi.org/10.1007/s10535-018-0785-4.
Zulfiqar, U., Ayub, A., Hussain, S., Waraich, E.A., El-Esawi, M.A., Ishfaq, M., Ahmad, M., Ali, N., Maqsood, M.F., 2022. Cadmium toxicity in plants: Recent progress on morpho-physiological effects and remediation strategies. J. Soil. Sci. Plant Nutr. 22 (1), 212–269. https://doi.org/10.1007/s42729-021-00645-3.